Eco-Friendly Basalt Fiber Reinforced Cement Composites (BFRC) Containing Waste Copper As Partial Replacement For Sand And Cement

Mohammed Najı Ahmed Abu Aeshah
Kastamonu University: Kastamonu Universitesi
Gökhan Kaplan (gkaplan@atauni.edu.tr)
Ataturk University: Ataturk Universitesi https://orcid.org/0000-0001-6067-7337

Research Article

Keywords: Copper slag, copper aggregate, basalt fiber, durability, sustainability

Posted Date: July 6th, 2021

DOI: https://doi.org/10.21203/rs.3.rs-563146/v1

Abstract

In this study, the use of copper slag and aggregate together with basalt fiber in cement-based composites was studied. It was aimed to contribute to the ecosystem by using copper waste, which is an environmental problem, in cement-based composites. In addition, the effect of basalt fiber on the strength and durability properties of composites was investigated. Taguchi optimization was carried out for cement-based composites. In this context, Taguchi L18 matrix was used. Copper slag was used at rates of 0, 7.5% and 15%, and copper aggregate at rates of 0, 25% and 50%. Basalt fibers of 6 and 12 mm length were used at the rates of 1%, 2% and 3%. The w/b ratios of the mixtures were chosen as 0.40, 0.50 and 0.60. Durability tests such as permeability, freeze-thaw and sulphate resistance with fresh and hardened mortar properties were performed on 18 different mixtures. In terms of the 7, 28 and 91-day flexural and compressive strength of the mixtures, the use of 1% of 6 mm long fiber in the mixtures with a w/b ratio of 0.40 provided more positive results. In terms of freeze-thaw resistance, it is necessary to use 3% of 6 mm long fiber in mixtures with 0.40 w/b. The use of 7.5% copper slag reduced the water penetration depth. The use of 15% copper slag in mixtures affected by sodium sulphate reduced the expansion values. Since the increase in the ratio of copper aggregate decreased the aggregate volume, it caused the drying shrinkage values to increase. As a result, it was observed that copper slag has a more positive effect than copper aggregate for the strength and durability of composites. However, by using 25% of copper aggregate by sacrificing some features, it can contribute to the environment and ecosystem. The use of basalt fiber with a length of 6 mm and a ratio of 1% increased the mechanical properties, while the use of 3% contributed significantly to the freeze-thaw resistance. It was determined that copper wastes contribute to the environment and ecosystem by using them instead of cement and aggregate.

Introduction

The construction of concrete infrastructures such as buildings, bridges, dams and roads in developing countries requires large amounts of materials obtained from natural resources. These developments in the construction sector increase the importance of natural resources over the next decade. Therefore, the construction sector has begun to adopt the concept of sustainability (Sharma and Khan 2018). While some countries are poor in terms of natural resources, developed countries have used these natural resources frequently in the construction sector. This situation led to a decrease in natural resources worldwide. In 2015 alone, 48.3 billion tons of aggregate was produced from natural resources (Freedoniagroup 2016). In addition, approximately 4000 MJ/t of energy is required for the grinding and calcination of raw materials in the Portland cement production process (Shi and Qian 2000). In addition to the energy used in cement production, high amounts of CO_2 emission are also generated and the environment is damaged (Edwin et al. 2016).

Industrialization and population growth, dumping or disposal of waste materials cause environmental problems (Chithra et al. 2016). The construction sector makes a great contribution to the disposal of these waste materials. In studies conducted in the literature, it has been determined that waste materials such as fly ash, rice husk ash, silica fume, blast furnace slag, other metal slags and recycled aggregate can be used in cement and concrete production (Ramanathan et al. 2013; Fallah and Nematzadeh 2017; Toklu and Şimşek 2018; Liu et al. 2019; Bayraktar 2021; Kaplan et al. 2021; Kaplan and Salem Elmekahal 2021).

Copper slag, which occurs as a byproduct, is about threefold of the production of copper metals. Since copper is used in many industries, copper mining activities are increasing day by day. As a result of the increase in copper need, copper slag comes out as waste material (Esmaeili and Aslani 2019). As the disposal of copper slag has become a concern for Environmental Protection agencies and governments, searches for possible alternatives to this waste material have begun (Mavroulidou 2017). Copper slag is mainly rich in Fe_2O_3, SiO_2 and contains various other oxide types, including Al_2O_3, CaO and MgO (Ramanathan et al. 2013; Chithra et al. 2016). In addition, copper slag may contain heavy metals that are harmful to the environment and ecosystem (Hagelüken 2006). Globally, approximately 68.7 million tons of copper slag

was released from the world copper industry in 2015. Figure 1 shows that China generates one third of the world's copper slag production, followed by Japan at 9%, Chile at 8% and Russia at 5%. Approximately 3.5% of the world's copper slag was formed in India with a production of 2.4 million tons in the same year (International Copper Study Group 2016).

The use of copper metal is gradually increasing at a rate of 7% per year for various applications and the waste from the product is increasing simultaneously. This waste needs to be disposed of or managed appropriately to achieve a sustainable environment. It is possible to dispose of these wastes from the copper industry by using them in the construction sector (Sharma and Khan 2018). The use of copper slag instead of cement and aggregate, which lead to the consumption of natural resources, was determined as an alternative solution (Tixier et al. 1997; Moura et al. 2007; Al-Jabri et al. 2011). Because its physical properties are similar to aggregate, copper slag is recommended to be used as aggregate in South Korea, Japan and India (Prem et al. 2018). It was also determined that copper slag can be used instead of cement in certain proportions (Shirdam et al. 2019). Studies in the literature showing that copper slag can be used as cement and aggregate are summarized in Table 1.

Table 1
The effect of copper slag on the strength and durability properties of cement-based composites

Study	Observations
Sharma and Khan (Sharma and Khan 2018)	It has been used instead of natural aggregate in SCC design.
Edwin et. al (Edwin et al. 2016)	They determined that the workability increased with the increase in the copper slag content.
Mobasher et. al (Mobasher et al. 1996)	They studied the effect of copper slag on cement hydration.
Arino et. al (Ariño and Mobasher 1999)	They determined that it is possible to replace copper slag with cement up to 15%.
Moura et. al (Moura et al. 1999)	It was determined that it can contribute positively to the mechanical properties of concrete (at optimum rate).
Ayano and Sakata (Ayano and Sakata 2000)	It extended the setting time of concrete.
Zain et. al (Zain et al. 2004)	They studied the effect of copper slag on compressive strength in concrete and mortars.
Al-Jabri et. al (Al-Jabri et al. 2006)	Similar strengths were obtained by using 5% instead of cement.
Khanzadi and Behnood (Khanzadi and Behnood 2009)	It increased the Schmidt hammer hardness by about 9%.
Najimi et. al (Najimi and Pourkhorshidi 2011)	It increased the sulphate resistance.
Najimi and Pourkhorshidi (Najimi et al. 2011)	It has reduced ASR expansions.
Ambily et. al (Ambily et al. 2015)	It was used as 100% filler material.
Thomas et. al (Thomas et al. 2013)	It was observed that it can be used instead of fine aggregate up to 60%.
Mavroulidou (Mavroulidou 2017)	Durability properties were improved
Prem and Ambiliy (Prem et al. 2018)	They used copper slag instead of fine aggregate.

Adding fiber to concrete can improve its mechanical properties and durability effectively. Three-dimensional randomly distributed fibers inhibit the initiation and expansion of cracks as well as reduce the stress intensity near the cracks. Fibers also increase the compression and flexural toughness of concrete (Al-Masoodi et al. 2016; Ghazy et al. 2016). Steel, glass,

carbon, polypropylene, polyvinylaccol, high density polyethylene fiber and basalt fiber are some fiber types used in concrete production. Basalt fibers have various advantages such as E-Modulus, specific strength, non-toxic, low cost, high temperature durability and high thermal insulation properties (Novitskii 2004; Quagliarini et al. 2012; Fiore et al. 2015). The chemical and mechanical properties of basalt fiber depend on the composition of the raw material. Different fiber composition and ratio affect thermal and chemical stability, as well as change mechanical and Physical Properties (Novitskii 2004). It has a very wide operating temperature range of -270 / + 750 ^{o}C (Morozov et al. 2001; Militký et al. 2002). The chemical structure of basalt fiber is almost dependent on glass.

The most important components of basalt fibers are SiO_2, Al_2O_3, CaO, MgO, Fe_2O_3 and FeO (Deák and Czigány 2009). Basalt fibers are chemically composed of pyroxene, clinopyroxene, olivine and plagioclase minerals (Dhand et al. 2015). Basalt fiber has excellent mechanical properties compared to other natural fibers (carbon and glass fiber, etc.). It has also become an ideal material for civil engineering applications due to its light weight, economical and environmentally friendly properties. These positive properties of basalt fiber make it more preferable to steel and carbon fibers (Ahmad et al. 2019). In addition, the risk of corrosion in steel fibers is also a significant disadvantage (Alnahhal and Aljidda 2018). Adding basalt fibers to the mixture can significantly reduce drying shrinkage while increasing deformation and energy absorption capacity, toughness index, flexural strength, and abrasion resistance (Dias and Thaumaturgo 2005; Li and Xu 2009; Jiang et al. 2010; Kabay 2014). It was observed that a strong adherence was formed between the cement matrix and the basalt fiber in the microstructure examined with SEM images (Jiang et al. 2014). Many studies have been conducted in the literature to determine the effect of basalt fiber on the fresh and hardened properties of concrete. Some of these studies are summarized in Table 2.

Table 2
Effects of basalt fiber on cement-based composites

Study	Observations
Zielinski and Olszewski (Zieliński and Olszewski 2005)	They stated that it reduces shrinkage.
Tumadhir (Tumadhir and Borhan 2013)	They observed that the tensile splitting strength increased.
High et. al(High et al. 2015)	It was observed that the modulus of rupture increased with fiber addition.
Wu et. al (Wu et al. 2015)	It was observed to be resistant to corrosion caused by ocean water.
Branston et.al (Branston et al. 2016)	They determined that the flexural strength increased substantially.
Algin et. al (Algin and Ozen 2018)	When used in optimum ratio, mechanical properties improve.
Niu et. al (Niu et al. 2020)	It was observed that it can contribute to chlorine penetration in optimum fiber content.
Liu et. al (Liu et al. 2020)	They determined the optimum fiber content in terms of mechanical properties as 2%.
Alnahhal and Aljidda (Alnahhal and Aljidda 2018)	They stated that early crack formation was prevented.
Elshafie and Whittleston (Elshafie and Whittleston)	The use of 0.1 and 0.5% fiber by volume increased the compressive strength.
Asprone et. al (Asprone et al. 2014)	It was observed that with the addition of fiber, the expansion in the mortar is reduced.
Fathima (Irine I .A 2014)	With the addition of 4 kg/m^3 fiber, the mechanical properties of concrete have improved.
Katkhuda and Shatarat (Katkhuda and Shatarat 2017)	They stated that basalt fiber can be used in concretes produced with recycled aggregate..
Sim et. al (Sim et al. 2005)	They observed that cement-based composites improved their properties.
Nasir et. al (Nasir et al. 2012)	It was observed that it is resistant to acid effect.

The Taguchi method minimizes the effects of uncontrolled factors while reducing the number of experiments. It is a powerful design method used in various engineering analyses to identify important factors and optimum conditions. This method is based on orthogonal design and uses the loss function, which is converted to a signal-to-noise (S/N) ratio, to calculate the deviation between actual experimental values and targeted values. A Taguchi sequence is an orthogonal design in which L levels of other factors are tested at least once for each level of the control factor (P-1) (Menten 1991; Davis and John 2018). The Taguchi method is an effective experimental design method that saves time and cost. The analysis of the S/N ratio is mainly based on three statistical characteristics. These are classified as (1) smaller-better, (2) bigger-better, and (3) Nominal-better. Three types of performance features are presented in the following equations (Fantous and Yahia 2020).

Bigger-better

$$S/N=-10Log_{10}[\sum_{i=1}^{n} y_{ij}^{2}] \quad (1)$$

Smaller-better

$$S/N=-10Log_10[\sum_{i=1}^{n}\frac{1}{y_{ij}^2}] \quad (2)$$

Nominal-better

$$S/N=-10Log_{10}[\sum_{i=1}^{n}(y_{ij}-m)^2] \quad (3)$$

Here, y_{ij} are experimental measurements for research responses, n and m are the number of repetitions and nominal value of a given measurement respectively. One of these methods is chosen according to the optimization purpose.

In this study, it was aimed to evaluate copper wastes that cause major environmental problems in basalt fiber-doped cement-based composites. It is aimed to find the optimal mixture for the effect of copper waste and basalt fiber on the strength and durability of cement-based composites.

Experimental Program

2.1. Materials

In this study, CEM I 42.5 R type cement in accordance with EN 197-1 (EN 197-1 2002) standard was used as a binder in the production of cement-based composites. The specific gravity of the cement is 3.13 and the Blaine value is 3300 cm^2/g. Copper slag with a specific gravity of 3.69 was used as cement replacement material. The Blaine value of the copper slag was measured as 3590 cm^2/g. Chemical properties and appearances of cement and copper slag are presented in Table 3.

Table 3 Chemical properties of cement and copper slag

Oxides	Cement	Copper slag
CaO	64,4	1,6
SiO_2	19,6	25.6
Al_2O_3	5,5	0,6
Fe_2O_3	2,9	69.1
MgO	2,1	0,2
SO_3	2,7	0,2
CuO	<0,01	1,3
LOI	2,1	-
Appearance		

Crushed stone aggregate and copper aggregates obtained by crushing from copper slags were used in the mixtures. Copper and crushed stone aggregate has 0–5 mm sieve aperture. The specific gravity of crushed stone and copper aggregates was determined as 2.66 and 3.13, respectively. The water absorption value of crushed stone aggregate was determined as 2.9%, and the water absorption value of copper aggregate was determined as 1.2. Particle distributions of crushed stone and copper aggregate are given in Fig. 2.

The copper slag, used instead of cement, is ground to cement fineness with a ball mill. The copper slag used instead of aggregate was crushed with the help of a stone crusher and brought to the size of crushed stone aggregate. Equipment used in grinding and crushing processes are given in Fig. 3.

6 and 12 mm long basalt fibers were used in the preparation of copper slag-doped cement based composites. The technical properties and appearances of basalt fibers are given in Table 4.

Table 4 Engineering properties of basalt fiber

Properties	Basalt fiber
Fiber type	Filament
Density (g/cm^3)	2,60
Length (mm)	6-12
Diameter (µm)	15
Young's modulus (GPa)	85
Tensile strength (MPa)	2800-3000
Melting point (°C)	~1350
Ultimate elongation (%)	~3
Color	Golden brown
 6 mm	 12 mm

For workability where the water/binder (w/b) ratios of the mixtures are different, a high range water reducer (HRWA) admixture called Glenium 51 was used. The high range water reducer (HRWA) admixture is based on polycarboxylate ether.

2.2. Mixture Properties

In the preparation of mixtures, the aggregate/binder ratio was chosen as 3. The water / binder ratio (w/b) consists of three different variables: 0.40, 0.50 and 0.60. Copper slag is replaced by both cement and aggregate. Copper slag used instead of cement was used in rates of 7.5% and 15%. Copper slag used instead of aggregate was used in 25% and 50% ratios. 6 and 12 mm long basalt fiber was added to the mixtures. Basalt Fiber was used in proportions of 1%, 2% and 3% by cement weight. The Taguchi L18 Matrix was used in the preparation of cement-based composites. The variables of the experimental study are given in Table 5 and the material quantities are given in Table 6.

Table 5
Variables of experimental study

Variables	Level 1	Level 2	Level 3
Fiber length (mm)	6	12	-
Fiber ratio (%)	1	2	3
W/B	0.40	0.50	0.60
Copper slag (%)	0	7.5	15
Copper aggregate (%)	0	25	50

Table 6
Design of the Taguchi L18 Matrix

Mixing Parameters						Quantities of Materials (g)					
Mix No,	Fiber Length (mm)	Fiber Ratio (%)	W/B ratio	Copper Slag (%)	Copper Agg. (%)	Cement	Copper Slag	Water	Limestone	Copper Aggregate	Fiber
1	6	1	0,4	0	0	450,00	0,00	180	1350,0	0,0	4,5
2	6	1	0,5	7,50	25	416,25	33,75	225	1012,5	337,5	4,5
3	6	1	0,6	15	50	382,50	67,50	270	675,0	675,0	4,5
4	6	2	0,4	0	25	450,00	0,00	180	1012,5	337,5	9,0
5	6	2	0,5	7,50	50	416,25	33,75	225	675,0	675,0	9,0
6	6	2	0,6	15	0	382,50	67,50	270	1350,0	0,0	9,0
7	6	3	0,4	7,50	0	416,25	33,75	180	1350,0	0,0	13,5
8	6	3	0,5	15	25	382,50	67,50	225	1012,5	337,5	13,5
9	6	3	0,6	0	50	450,00	0,00	270	675,0	675,0	13,5
10	12	1	0,4	15	50	382,50	67,50	180	675,0	675,0	4,5
11	12	1	0,5	0	0	450,00	0,00	225	1350,0	0,0	4,5
12	12	1	0,6	7,50	25	416,25	33,75	270	1012,5	337,5	4,5
13	12	2	0,4	7,50	50	416,25	33,75	180	675,0	675,0	9,0
14	12	2	0,5	15	0	382,50	67,500	225	1350,0	0,0	9,0
15	12	2	0,6	0	25	450,00	0,00	270	1012,5	337,5	9,0
16	12	3	0,4	15	25	382,50	67,5	180	1012,5	337,5	13,5
17	12	3	0,5	0	50	450,00	0,00	225	675,0	675,0	13,5
18	12	3	0,6	7,50	0	416,25	33,75	270	1350,0	0,0	13,5

2.3. Test Methods

Three samples were carried out in the experiments to determine the strength and durability properties of cement-based composites.

2.3.1. Fresh Mortar Properties and Unit Weight (UW)

Flow diameters of cement-based composites were determined according to ASTM C1437 (ASTM C1437 2020) standard. The flow diameters of mortars were determined by measuring in the X and Y direction. Since there are many parameters affecting the workability of the mixtures, the chemical additive ratio of each mixture was different. The plasticizer ratio was determined on the basis of 15 ± 3 cm flow diameter. Since the plasticizer ratio increased too much at low w/b ratios leads to segregation, the flow diameters of the mixtures with 0.40 w/b ratio were chosen lower values. The unit weights of the mixtures were determined in 50*50*50 mm cube specimens. Mortars were placed in the molds in two layers by compressing them with the help of a vibration table. Unit wights of the hardened mortars were determined after drying in an oven at 50 ^{o}C for 3 days. The sizes of the mortars were measured with the help of calipers and their volumes were determined approximately.

2.3.2. Compressive and Flexural Strength

Compressive and flexural strengths of cement-based composites were determined in 40*40*160 mm sized specimens. Mixtures were placed in the mold by compressing with two layers and a vibration table. The mechanical properties of the mixtures were determined according to the ASTM C348 and 349 standard (ASTM C349 2018; ASTM C348 2021). The three-point flexural strength test was first performed on the samples. The compressive strength was determined after flexural strength test. The compressive and flexural strengths of the mixtures were determined on the 7th, 28th and 91st days.

2.3.3. Sorptivity

Sorptivity properties of cement-based composites were determined in cube specimens of 50*50*50 mm and according to ASTM C1585 (ASTM C1585 2020) standard. Water penetration depth of the mixtures was measured until the 28th day. A water impermeability material with a height of 0.5 cm was applied to the side surfaces (surface in contact with water) of the mortars.

2.3.4. Drying Shrinkage

Drying shrinkage measurements were carried out in accordance with ASTM C 596 (ASTM C596 2018) standard. Mortar bars of 25*25*285 mm are used for drying shrinkage. 28-day pre-curing was applied to the drying shrinkage samples. The reason for the long pre-curing time is due to the copper slag used instead of cement. After the pre-curing process, the shrinkage values were measured on the 3rd, 7th, 14th, 21st, 28th, 35th, 42nd, 49th, 56th and 90th days.

2.3.5. Sulphate Resistance

The sulphate resistance of cement based composites was determined according to the ASTM C 1012 (ASTM C1012 2018) standard. However, instead of 5% Na_2SO_4, 10% Na_2SO_4 solution was used to speed up the process in determining the sulphate resistance. 25*25*285 mm sized mortar bars are used for sulphate resistance. The mortar bars were first cured for 28 days and then placed in the Na_2SO_4 solution. Length changes of cement-based composites were measured on the 3rd, 7th, 14th, 21st, 28th, 35th, 42nd, 49th, 56th and 90th days. The expansion and contraction behaviors were determined with the digital comparator in Fig. 4.

2.3.6. Freeze-Thaw Resistance

ASTM C 666 (ASTM C666 2003) standard was used for the freeze-thaw resistance of cement-based composites. After a 28-day curing process was applied to cement-based composites, freeze-thaw cycles were initiated. Freeze-thaw cycles were designated to be between − 20 /+4 ^{o}C. Samples with freeze-thaw resistance of 40*40*160 mm were produced. 50, 100 and 200 cycles were applied to the composites to determine the freeze-thaw effect. At the end of each cycle, compressive and flexural strength tests were applied to the samples.

Results And Discussion

3.1. Fresh State Properties and Unit Weights of Cement Based Composites

The amount of plasticizer of mixtures varies, since basalt fibers in different proportions and lengths are used. In addition, it was not possible to keep the amount of plasticizer constant since there are many factors affecting the workability. It was determined in preliminary tests that the main factor affecting the workability is basalt fiber. Figure 5 shows the factors affecting the plasticizer ratio.

As the fiber length increases, the plasticizer ratio increases. In the use of 12 mm long fiber, as the fiber ratio increases, the amount of plasticizer increases (Fig. 5a). In the case of increasing the fiber ratio from 1–3%, the plasticizer ratio increased approximately 55%. Similar situations were observed in 6 mm long fibers. However, the use of 2 and 3% fiber did not affect the amount of plasticizer much. If the fiber ratio was 2%, the plasticizer ratio increased about 115%. It is seen that less plasticizer ratio is used in short fibers. However, in short fibers, the increase in fiber ratio among themselves increases the plasticizer ratio more. In long fibers, this increase remains at lower levels. In the study conducted by Emdadi et al., workability losses occurred as PP fiber length increased (Emdadi et al. 2015). Workability decreases since the increase of fiber length increases the internal friction. Therefore, the plasticizer ratio should be increased.

Fig. 5 (b) shows the effect of copper wastes on the plasticizer ratio. The use of 25% copper aggregate in mixtures used 0% copper slag increased the plasticizer ratio, while the use of 50% copper aggregate decreased the plasticizer ratio relatively. Similar results were observed when using 15% copper slag too. The use of 25% copper aggregate increased the plasticizer rate while 50% copper aggregate reduced the plasticizer rate. In the use of 7.5% copper slag, the 25% copper aggregate content reduces the plasticizer rate. Generally, it has been observed that the use of copper slag increases the amount of plasticizer.

As seen in Fig. 6 (a), as the w/b ratio increases, the plasticizer ratio decreases. In addition, as a result of the increase in fiber ratio, the rate of plasticizer generally increases. In the case of decreasing of w/b ratio from 0.60 to 0.40 at 3% fiber ratio, the plasticizer ratio increased approximately 11 times. Increasing of the fiber ratio has a great effect on workability.

Increasing copper slag at low w/b ratio (0.40) increases the plasticizer ratio more. If the w/b ratio is 0.50 and 0.60, the copper slag ratio does not affect the plasticizer ratio very much. If the copper slag is 7.5% and over in mixtures with a ratio of 0.40 w/b, the amount of plasticizer is over 2% (Fig. 6b). It was observed that copper slag affects the amount of plasticizer more at low w/b ratios. This situation is thought to be due to the paste volume.

As can be seen in Fig. 7(a), if the fiber ratio is 2%, the flow diameters of the mixtures produced from 6 and 12 mm long fibers increase. The reason for this increase is the use of more plasticizers in mixtures with 2% fiber ratio. Using 3% fiber in mixtures of 6 and 12 mm long fibers reduced the flow diameters. In the case of using 3% fiber, more plasticizer was used, but the expected improvement in the flow diameters of the mortars could not be observed. This is because, with the increase in the number of fibers, the internal friction increased and the flow diameters decreased. Since more plasticizer was used in the mixtures produced from 12 mm long fibers, the flow diameters were higher. In the case of preferring of a fiber of 12 mm length in mixtures with 3% fiber, the flow diameter was increased by approximately 10%. However, this is related to the excess plasticizer used. It was observed that the optimum ratio for short and long fibers is 2%. As the PP fiber content increased at a constant w/b ratio, the slump values of concrete were decreased by Hasan et al. (Hasan et al. 2019). Qin et al. used different proportions of basalt fiber in the mixtures they produced from magnesium phosphate cement. As a result of the increase in basalt fiber content, the workability of the mixtures decreased (Qin et al. 2018). More cement paste is needed to wrap around filament fibers with large surface areas, and the water absorption capacity of these fibers also negatively affects the workability (Dias and Thaumaturgo 2005; Chen and Liu 2005). In their study,

Jalasutram et al. increased the amount of plasticizer together with the basalt fiber content, but could not eliminate the loss of workability (Jalasutram et al. 2017). Similar results were observed in the study conducted by Kabay, with the content of basalt fiber, the amount of plasticizer was increased and the workability was arranged in this way (Kabay 2014).

When the copper slag is used at the rate of 7.5%, the flow diameter increases with the increase in copper aggregate (Fig. 7b). If 7.5% copper slag is used, the flow diameters of the mixtures vary between 151–185 mm. The flow diameters of mixtures containing 0 and 15% copper slag showed similar properties. Especially in the case of using 25% copper aggregate, the flow diameters increased, while the use of 50% copper aggregate decreased the flow diameters. Since more plasticizer was used, this situation was observed when 25% copper aggregate was used in mixtures with 0 and 15% copper slag. In the mixtures containing 50% copper aggregate, relatively less plasticizer was used and the flow diameters decreased. In addition, the angled structure of the copper aggregate like crushed stone aggregate increased the internal friction and affected the workability more negatively. Therefore, the amount of plasticizer was also increased. The flow diameters of the mixtures containing 15% copper slag vary between 133–142 mm. Khanzadi and Behnood increased the slump values of concretes by using copper aggregate in their study (Khanzadi and Behnood 2009). Al jabri et al. produced concretes using different proportions of copper aggregate. As the copper aggregate increased, the slump values of the mixtures increased (Al-Jabri et al. 2011). This positive effect of copper aggregate was stated by some researchers because of its low water absorption rate (Ishimaru et al. 2005; Sharma and Khan 2017a). The high specific gravity of copper aggregate generally increases the slump values (dos Anjos et al. 2017). Najimi et al used copper slag by replacing it with cement up to 15%. The use of 5% copper slag increased the slump value relatively. 10% and 15% copper slag did not cause any loss of workability. The absence of slump loss was explained by the high specific gravity of the copper slag (Najimi et al. 2011). Onuaguluchi and Eren reported that the flow diameters decreased with the increase of copper slag in their study (Onuaguluchi and Eren 2013).

Figure 8 shows the effect of w/b ratio on the flow diameter. If the W/B ratio is 0.40, the flow diameter varies between 122–182 mm. Due to the low W/B ratio, the variability in the amount of plasticizer used to improve the workability of the mixtures was reflected in the flow diameter. When the W/B ratio was 0.50, mixtures with a flow diameter of 129–169 mm were obtained. In mixtures with a ratio of 0.60 w/b, the change in flow diameter was less and values between 135–160 mm were observed. As the relative w/b ratio increases, the flow diameters decrease. The reason for this can be explained by the amount of plasticizer used. As the W/B ratio increased, the amount of plasticizer decreased and in this case the flow diameters partially decreased.

Figure 9 shows the flow diameter of cement based composites in which fiber and copper waste are used. The flow diameters of the mixtures vary between 117–199 mm. The lowest flow diameter was obtained in mixture number 1, and the highest flow diameter was obtained in mixture number 13. It was also observed that there was some segregation in the mixture numbered 13. Some segregation occurred due to the plasticizer ratio being 2.75%.

Fig. 10 shows the effects of fiber and copper wastes on unit weight. As the fiber ratio in the miztures increases, the unit weight values of the composites decrease. This applies to both 6 and 12 mm long fibers. Unit weight values decreased as the fibers increased the internal friction during insertion into the mold (Fig. 10a). If the fiber ratio is 2% and over, the unit weight values of the mixtures fall below 2400 kg/m^3. When 12 mm long fibers were used at 3% instead of 1%, unit weight decreased by about 5%. The change in fiber ratio affected the unit weight values, even a little. Using 1 and 3% of 12 mm long fibers further reduced the unit weight. As the basalt fiber content increased in the study conducted by Qin et al. the unit weight of concrete decreased (Qin et al. 2018). Similar results were observed with mixtures made with glass fiber (Tassew and Lubell 2014; Hong and Lubell 2015). Hanafı et al. observed that unit weight values did not change much with the increase in fiber ratio in cement pastes that they obtained by using different proportions of basalt fiber (Hanafı et al. 2020). In the study conducted by Borhan, as the basalt fiber content increased, the unit weight values of the concrete decreased (Borhan 2012).

When 7.5% and 15% copper slag is used, the unit weight values increase as the copper aggregate content increases (Fig. 10b). However, this situation was not observed in mixtures without copper slag. The unit weight value of the mixtures without copper slag did not changed much, approximately 2350 kg/m^3 value was obtained. In the case of using 7.5% and 15% copper slag, the unit weight values were between 2400–2500 kg/m^3 as a result of the increase in copper aggregate. Especially when 50% copper aggregate and 15% copper slag were used, the unit weight value of the mixtures was approximately 2500 kg/m^3. No significant relationship was observed between the flow diameters and the unit weight values of mixtures produced from copper waste. This is because copper slag and copper aggregate have high specific gravity. Although the workability of the mixtures is bad, the unit weight values increased due to their high specific gravity. Anjos et al. stated that unit weight values increased as a result of the increase in the aggregate content in the concrete they produced using copper aggregate (dos Anjos et al. 2017). Khanzadi and Behnood used copper slag instead of aggregate and the unit weight values of concretes increased with the increase in slag ratio (Khanzadi and Behnood 2009). In the study conducted by Al jabri et al. copper slag was evaluated as aggregate. As the copper slag ratio increased, the unit weight values of the concrete increased. The unit weight values of concretes in which 100% copper slag was used were determined to be approximately 2700 kg/m^3 (Al-Jabri et al. 2009). Najimi et al. used copper slag up to 15% instead of cement and achieved increases in the unit weight of the mixtures (Najimi et al. 2011). Similar results were observed in the study conducted by Gupta et al. (Gupta et al. 2017). Studies indicated that when copper slag is used instead of aggregate and cement, the unit weight increases. This is explained by the fact that copper wastes have a higher specific gravity than both aggregate and cement.

As seen in Fig. 11, as the w/b ratio increases, the unit weight values of the mixtures decrease. The unit weight values of mixtures with a w/b ratio of 0.40 vary between 2300–2570 kg/m^3. In mixtures with a W/B ratio of 0.50, the unit weight values vary between 2250–2390 kg/m^3. The unit weight values of mixtures with a ratio of 0.60 w/b are generally below 2400 kg/m^3. Since increase of the w/b ratio in the mixtures increases water content the unit weight value of the mixtures decreases. The unit weight values over 2500 kg / m^3 were obtained in mixtures with a ratio of 0.40 w/b.

3.2. Compressive and Flexural Strength of Cement Based Composites

Figure 12 shows the effect of fiber and copper wastes on the flexural strength of 7, 28 and 91-day mixtures. The flexural strength of the basalt fiber doped mixtures varies between 4.5–6.8 MPa (Fig. 12a). If 1% and 3% of 6 mm long fibers are used, the flexural strength is 6 MPa and over. However, when the fiber ratio was 2%, the flexural strength decreased. The increase in fiber ratio in the use of 12 mm long fibers increased the flexural strength. However, when 12 mm long fiber was used, the flexural strength did not exceed 6 MPa. The use of 6 mm long fiber increased the 7-day flexural strength relatively more than the 12 mm fiber.

When the 28-day flexural strength is examined, the increase in the fiber ratio in the use of 6 mm long fiber increases the flexural strength. However, when the fiber length is 12 mm, the increase in the fiber ratio decreased the flexural strength (Fig. 12a). The 28-day flexural strength of the mixtures generally exceeded 8 MPa with the effect of hydration. When 3% of 6 mm long fibers were used, the 28-day flexural strength was found to be approximately 8.8 MPa. As a result of the increase in fiber ratio, negligible decreases occur in flexural strength. In the case of using 2 mm long fiber at 3% instead of 1%, approximately 4% strenght loss was occured.

As seen in Fig. 12a, 91-day flexural strength generally improves as the fiber ratio increases. Strength loss occurred when only 2% of 12 mm long fibers were used. However, this strength loss value was approximately 13%. Similar properties were observed when 1% and 2% of 6 mm long fibers were used. It is seen that 91-day flexural strength is generally over 9 MPa. In terms of flexural strength of 28 days, it is seen that using 3% of 6 mm long fibers is more positive.

Borhan et al. stated in their study that the ratio of basalt fiber decreases the tensile splitting strength in some intermediate values, but increases it at some rates (Borhan 2012). However, losses in tensile splitting strength remained at negligible levels. Kabay used 2% and 4% basalt fiber in the concrete in his study. It was observed that the higher the rate of basalt fiber, the higher the flexural strength (Kabay 2014). Qin et al found similar results in their study and stated that as the rate of basalt fiber increases, the tensile splitting strength increases (Qin et al. 2018). In the study of Hanafi et al., the use of basalt fiber up to 0.75% generally increased the flexural strength, while the use of 1.5% basalt fiber decreased the flexural strength (Hanafi et al. 2020). These different behaviors in flexural strength may be due to the tendency of the fibers to coagulation.

Since basalt fiber is composed of SiO_2 and CaO, it is expected to show better mechanical performance. C-S-H gel formation provides a higher compressive and flexural strength. In addition, basalt fibers have an amorphous structure. This helps to form a densified matrix with homogeneous basalt fiber distribution in the cement paste. Saloni et al. (Saloni et al. 2020) reported that basalt fiber acts as an aggregate and increases strength more when strong matrix properties are formed. Similar results were observed in other studies (Pehlivanlı et al. 2016; Sadrmomtazi et al. 2018; Ralegaonkar et al. 2018; Chidighikaobi 2019).

Figure 12b shows the effect of copper wastes on the flexural strength properties. It is seen that the 7-day flexural strength varies between 4.2-7.0 MPa. On the 7th day, the highest bending strength (~ 7.0 MPa) was observed in mixtures using 7.5% copper slag but not using copper aggregate, and mixtures using 15% copper slag and 25% copper aggregate. The increase in copper aggregate in 7-day mixtures generally led to a decrease in flexural strength.

In the 28-day flexural strength, the increase in the copper aggregate content of the mixtures using 15% copper slag provided an increase in strength. In the case of using 7.5% copper slag, the increase in copper aggregate decreased the flexural strength. The flexural strength of mixtures without using copper slag increased only at 25% copper aggregate content. In the case of using 50% copper aggregate, the 28-day flexural strength decreased by approximately 15%. The 28-day flexural strength of the mixtures varies between 7-8.55 MPa. In terms of 28-day flexural strength, the most suitable mixture ratios were determined as 7.5% copper slag 0% copper aggregate or 15% copper slag 25% copper aggregate.

When the 91-day flexural strength is examined, in mixtures containing 0 and 7.5% copper slag, as the copper aggregate increases, the flexural strength decreased. In the case of being 15% of copper slag, the 25% copper aggregate increased the flexural strength by approximately 29%. The mixture with 50% copper aggregate and the mixture without copper aggregate showed similar properties. It is observed that the 91-day flexural strength varies between 8-11.5 MPa. The highest flexural strength was obtained in mixtures without 7.5% copper slag and copper aggregate. The flexural strength of the mixtures without copper aggregate and slag was approximately 11.5 MPa.

In the study conducted by Anjos et al., copper aggregates used instead of aggregate reduced the tensile strength (dos Anjos et al. 2017). Some studies reported that by using copper slag in place of fine aggregate, the compressive and tensile strengths are significantly higher than control mixes, almost in line with those of normal concrete (Hwang and Laiw 1989; Shoya et al. 1997; Khanzadi and Behnood 2009). In the study conducted by Al Jabri et al., when copper slag is used instead of aggregate, flexural strength decreases at some rates and increases at some rates (Al-Jabri et al. 2011). Wu et al. stated in their study that with the increase of copper slag ratio, the flexural strength decreases and the strength loss is due to excessive trapped water (Wu et al. 2010a).

Moura et al. used 10% copper slag instead of cement and observed a decrease in flexural strength (Moura et al. 1999). Antonio and Mobasher determined the flexural toughness by using 10% copper slag in concretes with 0.50 w/b ratio. It was observed that the flexural toughness decreases when copper slag is used instead of cement (Ariño and Mobasher 1999). In the study conducted by Onuaguluchi and Eren, copper slag used instead of cement by 10 and 15% decreased the flexural strength (Onuaguluchi and Eren 2013). The reason for the loss of strength is due to copper slag, which has less

reactivity compared to cement (Onuaguluchi and Eren 2012). In the study conducted by Gupta et al., flexural strength increased when copper slag was used instead of cement (Gupta et al. 2017).

As seen in Fig. 13, as the w/b ratio increases, the flexural strength of the mixtures decreases. The increase in the w/b ratio at all test times affects adversely the flexural strength. As a result of the increase in hydration period, the flexural strength increases. Especially on the 91st day, the flexural strength of the mixtures is 8 MPa and over. When the w/b ratio is increased from 0.40 to 0.60 in 28-day mixtures, the flexural strength decreases by approximately 25%. In the case of increasing the w/b ratio from 0.50 to 0.60 in 28-day samples, some strength development was observed.

Figure 14 shows the compressive strengths of mixtures obtained from basalt fiber and copper waste at different times. The use of 6 mm long fiber in 7-day compressive strength provided more positive results (Fig. 14a). In the use of 6 mm long fiber, choosing 1% and 3% fiber increases the compressive strength. The use of 2% fiber reduced compressive strength by 11%. The use of 12 mm long fiber also decreased the compressive strength relatively compared to the use of 6 mm long fiber. If 12 mm long fiber is used, the increase in fiber ratio decreases the compressive strength. It was observed that 7-day compressive strength varied between 39.8–45.8 MPa. It is more appropriate to use 1% or 3% of 6 mm long fibers in 7-day compressive strength.

It is seen that the fiber properties do not cause a significant increase or decrease in 28-day compressive strength. It is seen that thecompressive strength is between 49.2–54.1 MPa (Fig. 14a). It is observed that when 6 mm long fiber is used, 2% of it causes strength loss. However, it is seen that this strength loss is a small value as 6%. As the fiber ratio increases in the mixtures produced from 12 mm long fibers, the compressive strength decreases. Therefore, it has been determined that the optimal ratio is 1%, which provides the value of 52.6 MPa.

In 91-day mixtures, the increase in hydration process contributed to fiber-matrix adherence. In particular, using 1% of 12 mm long fibers has increased the compressive strength to approximately 80 MPa. However, the use of 2% and 3% fiber reduced the compressive strength by approximately 30%. In the case of using 6 mm long fiber, different results were obtained from other experiment days. Using 2% of the 6 mm long fiber increased the compressive strength relatively slightly. Compressive strength varies between 57.8–59.7 MPa in the use of 6 mm long fiber. The optimum mixture ratio in terms of 91-day compressive strength was the use of 1% of 12 mm long fiber. Similar results were observed in the study conducted by Borhan et al. and as a result of the increase in the ratio of basalt fiber, the compressive strength of some mixtures decreased (Borhan 2012). Dias and Thaumaturgo stated that the addition of 1.0% basalt fiber by volume reduced the compressive and tensile splitting strength of concrete by 26.4% and 12%, respectively. They also stated that concretes with lower fiber content (0.5% by volume) showed negligible changes in compressive and tensile splitting strength compared to non-fibrous concrete (Dias and Thaumaturgo 2005). In the study conducted by Kabay, the increase in basalt fiber ratio at low w/b ratio (0.45) decreased the compressive strength. However, the increase in fiber ratio at high w/b ratio increased the compressive strength (Kabay 2014). In the study conducted by Qin et al., the increase in basalt fiber ratio increased the compressive strength. Concretes with a compressive strength of about 80 MPa were obtained on the 28th day (Qin et al. 2018). In general, the addition of basalt fibers to the mixture increases the load-bearing capacity of composites. This increase in performance can be explained by the adherence between fiber-matrix (Simões et al. 2017). Sun et al. stated that the addition of basalt fiber up to 2% by volume increases the compressive strength, but adding more fiber affects the strength negatively (Sun et al. 2019). In the study conducted by Jalasutram et al., as the basalt fiber content increased, the compressive strength of concrete decreased (Jalasutram et al. 2017). The addition of basalt fibers did not provide a significant improvement in the dynamic compressive strength of the geopolymer concrete, but improved deformation and energy absorption capacities significantly (Li and Xu 2009). Jiang et al showed that the addition of basalt fibers to the mixture increased the compressive and flexural strengths in the early hydration period significantly (Jiang et al. 2010).

Figure 14 (b) shows the effect of copper wastes on compressive strength. In 7-day mixes, copper slag and aggregate generally reduce the compressive strength. In particular, using 50% copper aggregate in mixtures without copper slag reduced the compressive strength by approximately 48%. The use of 50% copper aggregate in mixtures using 7.5% copper slag reduced the strength loss. In mixtures using 15% copper slag, the use of 25% copper aggregate increased the compressive strength and a compressive strength of approximately 45 MPa was obtained. It has been observed that the optimum ratio for 7-day compressive strength is 7.5% copper slag and 0% copper aggregate.

It is seen that the 28-day compressive strength of the mixtures varies between 34.7–69.1 MPa (Fig. 14b). Generally, the increase in copper slag and aggregate reduces 28-day compressive strength. An increase in strength was observed in mixtures using only 15% copper slag and 25% copper aggregate. It is seen that 7-day and 28-day compressive strength are parallel to each other. Compressive strength of approximately 70 MPa was obtained in mixtures where copper waste is not used.

91-day Compressive strength was observed to be similar to other experiment days. Compressive strength of 90 MPa and over was obtained, especially in mixtures without copper waste. If the copper aggregate is 50% in mixtures without copper slag, the compressive strength is reduced by approximately 53%. With the increase in copper slag, the rate of strength loss caused by copper aggregate is reduced. The compressive strength of the mixtures in which 15% copper slag and 25% copper aggregate were used was over 60 MPa value. It was observed that it was possible to produce high-strength cement based composites with these rates.

In the study conducted by Anjos, copper slag was used instead of aggregate and the increase in slag ratio decreased the compressive strength of concrete (dos Anjos et al. 2017). Khanzadi and Behnood used copper slag as aggregate in their work. They observed that copper slag used as aggregate increased the compressive strength. The reason for the strength increase was explained by the strength of the copper slag aggregate. They also argued that copper slag aggregates had better adherence to the matrix than chalk (Khanzadi and Behnood 2009). In their study, Al Jabri et al. obtained strength increase by using copper slag instead of aggregate (Al-Jabri et al. 2011). Wu et al claimed that copper slag grains improve the cohesion of the concrete matrix thanks to their angular sharp edges. Due to its rough surface, the adherence between cement paste and aggregate increases. The angular sharp edges of the copper slag grains reduce the negative effects of fine aggregate to some extent and thus have the ability to further improve the cohesion of the concrete. In addition, the glassy surface texture of copper slag grains has a negative effect on cohesion. The low water absorption properties of copper slag cause excess water in the concrete. In high copper slag content, excessive bleeding may occur. This situation may cause micro voids or capillary voids in the concrete and lead to a decrease in concrete quality. Therefore, the strength of concrete with low copper slag content can be improved by the positive effect of copper slag, but if the copper slag content exceeds 40%, the strength of the concrete can be significantly reduced by a reduction in the effective cohesion (Wu et al. 2010a, b).

Mobasher et al. and Tixier et al. examined the effects of copper slag on cement hydration. Copper slag up to 15% by weight was used as a pozzolanic reaction activator with up to 1.5% hydrated lime in Portland cement replacement. The results showed a significant increase in compressive strength for up to 90 days of hydration. In addition, a decrease in capillary porosity and an increase in gel porosity were observed (Mobasher et al. 1996; Tixier et al. 1997). Moura et al. suggested that copper slag can be a potential alternative to additives used in concrete and mortars (Moura et al. 1999). Al Jabri et al. increased the compressive strength by using 5% copper slag in concretes with 0.50 w/b ratio (Al-Jabri et al. 2006). Zain et al. searched the use of copper slag in different proportions instead of cement. They found that copper slag extends the setting time of mortars and reduces the compressive strength. They stated that the optimum rate of replacement should be between 5-7.5% (Zain et al. 2004). In the Onuaguluchi and Eren's studies, while the strength increase up to 5% was achieved in the copper slag used instead of cement, strength loss was observed in a higher rate. Ranganath et al. (Ranganath et al. 1998) demonstrated that large particles are less reactive in cement mixtures and the delay of cement hydration due to the presence of Cu (II) ions was stated by Hashem et al. (Hashem et al. 2011).

Figure 15 shows that the compressive strength of mixtures decreases as the W/B ratio increases. Increase in w/b ratio on all test days decreases compressive strength. On the 91st day, the compressive strength of mixtures with different w/b ratio varies between 43–75 MPa. On the 28th day, the compressive strength of mixtures with a rate of 0.40 w/b exceeded 50 MPa, on the 91st day, mixtures with a ratio of 0.40 and 0.50 w/b exceeded 50 MPa. It was determined that mixtures with 0.60 w/b ratio do not exceed 50 MPa.

As seen in Fig. 16, the flexural strength of the mixtures increases as the compressive strength increases. Although the R^2 coefficient between compressive and flexural strength is 0.65, the increase in compressive strength generally increases the flexural strength.

In Fig. 17, the cross-sections for aggregate distribution of copper aggregate doped and undoped composites for which flexural strength tests have been applied are given. In Fig. 17 (a), it is seen that the aggregates with black color are the aggregates obtained from copper slag. It is also seen that the copper aggregates are homogeneously distributed.

3.3. Sorptivity Properties of Cement-Based Composites

Figure 18 shows the time-dependent water penetration depth of mixtures produced from 6 mm long fibers.

In Fig. 18, the highest water penetration depth was observed in the mixture numbered 3 in the early days of the sorptivity test. It is observed that the water penetration depth of the mixture number 3 increased in the following process. The reason for the high water penetration depth of the mixture numbered 3 is that the w/b ratio is 0.60. In addition, 50% copper aggregate is also effective in this process. The fact that the fiber content in the mixture number 3 is 3% is another factor that increases the water penetration depth. Since the w/b ratio of mixtures numbered 9 and 6 is 0.60, their water penetration depth is higher than other mixtures. The water penetration depth of the mixtures numbered 3,6,8 and 9 at the end of the 28th day varies between approximately 1.5–1.8 mm. Although the w/b ratio of the 8th mixture was 0.50, the fact that the fiber content was 3% led to an increase in the water penetration depth. The water penetration depth of the mixture number 1 is less than 0.6 mm. The w/b ratio of the mixture number 1 is 0.40 and the fiber content is 1%. With the decrease in the W/B ratio, water treatment depth generally decreases. The water penetration depth of the mixtures numbered 4 and 7 with a w/b ratio of 0.40 was determined as approximately 0.8 mm. The water penetration depth of the mixture number 6 increases continuously over time. It is estimated that this occurs because the 15% copper slag used in mixture number 6 reduces the content of the paste. On the other hand, in mixtures numbered 5 and 7, using 7.5% copper slag, the water penetration depth has not increased much since the 8th day. Since the copper aggregate content of the mixtures numbered 3 and 9 is 50%, it is observed that the depth of water penetration of the mixtures is higher. The use of copper aggregate, which has a higher specific gravity than crushed stone aggregate, increases the porosity of the mixtures. In this case, the water penetration depth of the mixtures can increase. In Fig. 19, the water processing depths of the blends produced with 12 mm long fibers are given.

The use of 12 mm long fibers generally reduced the depth of water penetration (Fig. 19). However, the increase in the w/b ratio increases the water penetration depth of the mixtures. Especially, the water penetration depth of the 18 numbered mixture with a w/b ratio of 0.60 and fiber content of 3% was found to be approximately 1.6 mm. Similar results were observed in the mixture number 12. The water penetration depth of the mixture numbered 12 with a W/B ratio of 0.60 and a copper aggregate ratio of 25% was found as 1.46 mm. Although the w/b ratio of the mixture number 17 was 0.50, the fact that the fiber content was 3% and the copper aggregate content was 50%, increased the depth of water penetration greatly. In addition, although the w/b ratio of the mixture numbered 10 is 0.40, since the copper aggregate content is 50%, the water penetration depth exceeded 1.20 mm. The water penetration depth of the mixture number 11 is less than 0.60 mm. Because no copper slag and aggregate are used in the mixture number 6. Capillar voids are thought to be less due to the fact that the paste volume and aggregate volume do not decrease. At the beginning of the experiment, it is seen that the mixture numbered 10 has a greater water penetration depth. The lowest water penetration depth was also observed in

the 11th mixture. On the 28th day, the water penetration depth of the mixture numbered 18 is 63% more than the mixture number 11.

As a result, the minimum water penetration depth was obtained as 0.54 mm in the mixture number 1. The w/b content of the mixture number 1 is 0.40 and the fiber content is 1%. In addition, copper wastes were not used in its structure. The maximum water penetration depth value was obtained as 1.77 mm in the mixture numbered 6. The fiber content of the 6th mixture with a W/B value of 0.50 is 2%. The 28-day compressive strength of the mixture numbered 6, in which no copper aggregate is used but 15% copper slag is used, is 37.91 MPa. Generally, mixtures with low compressive strength have more water penetration depths. It is thought that this situation is caused by the copper slag and aggregate used in the mixtures.

Nagarajan et al. used basalt fiber up to 0.25% in lightweight concretes. Sorptivity coefficients of concretes increased with the increase in basalt fiber ratio (Nagarajan et al. 2020). Basalt fiber was used up to 0.20% by volume in the study conducted by Niu et al. As the basalt fiber ratio increased, the water penetration depth of the concretes increased (Niu et al. 2020). When the fiber content is too high, the fibers are not distributed homogeneously, they overlap in the matrix and coagulation occurs, thus causing an increase in the coarse spaces between the fibers. As a result, higher water absorption occurs (Niu et al. 2020). In the study by Karthikeyan et al., basalt fiber was used up to 1% by volume. While the increase in basalt fiber ratio in some mixtures decreased the sorptivity coefficient, in some mixtures sorptivity coefficient increased (Karthikeyan et al.). In the study conducted by Adesina et al., 4% and 8% basalt fiber was used in concrete production. As a result of the increase in basalt fiber ratio, the water penetration depth of the mixtures also increased (Adesina et al. 2020).

In high performance concrete, sorptivity was reduced by using 40% copper slag as fine aggregates and 2% nanosilis as cement replacement (Chithra et al. 2016). Sharma and Khan used copper slag instead of aggregate and showed that sorptivity was better than control concrete (Sharma and Khan 2017a, b, 2018). In the study by Geetha et al., as the copper slag content increased, sorptivity values decreased (Geetha and Madhavan 2017). In the study by Gupta and Siddique, copper slag used instead of fine aggregate generally reduced sorptivity values (Gupta and Siddique 2020). Rajasekar et al. used copper slag instead of aggregate up to 100% and determined that capillarity values decreased (Rajasekar et al. 2019).

Sorptivity properties of mixtures obtained by using copper slag instead of cement were not studied much. However, as copper slag is effective on the paste volume, its effect on sorptivitycan be explained in this way. Sorptivity values generally decrease as a result of the increase in paste volume. There are many studies on this in the literature (Kolias and Georgiou 2005; Chen et al. 2014; Zhong and Wille 2015; Chu 2019).

3.4. Drying Shrinkage Properties of Cement Based Composites

Figure 20 shows the drying shrinkage time-dependent behavior of the mixtures produced from 6 mm long fibers. Drying shrinkage measurements were performed up to the 91st day after 7-day of water treatment.

Among the mixtures, the lowest shrinkage value (for 91 days) was obtained with the mixture numbered 1 as $1568x10^{-6}$. No copper slag and aggregate were used in the 1 mixture with a W/B ratio of 0.40. The shrinkage value of the other mixture (number 4) with a w/b ratio of 0.40 was also under $2000x10^{-6}$. Although the w/b value of the mixture numbered 7 was 0.40, the shrinkage value increased relatively and exceeded the value of $2000x10^{-6}$. Although the fiber content of the mixture numbered 7 was 3%, it did not show a very distinctive behavior in reducing drying shrinkage. The highest shrinkage value was obtained in the mixture numbered 9 with a w/b ratio of 0.60 and a copper aggregate ratio of 50%. The shrinkage value of mixture number 9 on the 91st day was measured as approximately $3500x10^{-6}$. The shrinkage values of the mixtures with 3% fiber content were over $2000x10^{-6}$. The shrinkage values of the mixtures with 2% fiber content were generally under $2000x10^{-6}$. The increase in fiber ratio generally increased the shrinkage value. The shrinkage values of the mixtures numbered 3, 6 and 8 with 15% copper slag were determined to be close to each other. The use of

copper aggregate generally increases the drying shrinkage values. Because the aggregate volume decreases and therefore the drying shrinkage increases.

Figure 21 shows the drying shrinkage time-dependent behavior of the mixtures produced from 12 mm long fibers. The lowest shrinkage values were observed in mixtures numbered 10, 11 and 12. The common point of these mixtures is that they have 1% fiber ratio. Drying shrinkage values increase in fiber ratios after 1%. The drying shrinkage values of the mixes numbered 14 and 15 with 2% fiber ratio approached approximately $4000x10^{-6}$. The w/b ratio of the mixture numbered 14 is 0.5 and the copper slag is 15%. The w/b ratio of the mixture numbered 15 is 0.60 and the copper aggregate content is 25%. In addition to the W/B ratio, the increase in copper slag and aggregate ratio increased the drying shrinkage behavior. Although the w/b ratio of the mixture numbered 18 was 0.60, the shrinkage value was measured as $3344x10^{-6}$. It is thought that the shrinkage value is reduced by 3% fiber used.

Increasing fiber length generally increased the drying shrinkage values of the mixtures. Mixtures using 12 mm long fibers generally have lower unit weight values. This situation indicates that the mixtures are more porous. It was determined that drying shrinkage values increased due to the porous structure. It is also known that mixtures with high compressive strength cause less shrinkage. Generally, high shrinkage values were observed in some mixtures with high fiber ratio, as the increase in fiber ratio reduces the compressive strength. The shrinkage value in mixtures numbered 13 and 17 with a copper aggregate content of 50% was measured as approximately 3500x10-6. Since the copper aggregate content decreases the total aggregate content, it generally increased the drying shrinkage values. In addition, the increase in w/b ratio also increased the drying shrinkage values. However, in some cases the high fiber content reduced this disadvantage.

Valeria and Nardinocchi stated that drying shrinkage can be reduced by fiber reinforcement in cement-based composites (Corinaldesi and Nardinocchi 2016). Jiang et al. observed in their study that the drying shrinkage at an early age is reduced by the addition of basalt fiber (Jiang et al. 2010). Punurai et al. stated in their study that as the basalt fiber content increases, the drying shrinkage decreases. They stated that basalt fiber acts as a micro-aggregate due to its reactivity and therefore its shrinkage values decrease (Punurai et al. 2018). Jiang et al. obtained lower shrinkage values than the control mixture using the basalt fiber (Jiang et al. 2016). Ruijie et al used 0.1% and 0.3% basalt fiber in their study. The increase in basalt fiber ratio increased the shrinkage value of some mixtures, but generally the shrinkage values decreased (Ruijie et al. 2017). In the study conducted by Li et al., it was observed that drying shrinkage increased in some mixtures containing basalt fiber (Li et al. 2020). In addition, studies indicated that drying shrinkage is mainly affected by transition pores with diameters less than 50 nm (Zhong and Zhang 2020). This situation also shows the effect of w/b ratio on drying shrinkage. The researchers stated that as the curing time increases, the decrease in the shrinkage rate is related to the rate of water loss. The drying shrinkage rate of basalt fiber doped mixtures was lower than that of control concrete during all curing times. This result shows that basalt fiber has a positive effect in reducing the drying shrinkage rate. There are three reasons for this result: (1) Adding fiber to the mixture increases the tensile strength of the concrete matrix, which physically contributes to restrictive shrinkage. (2) With the fiber addition, crack development is prevented by the bridging effect and (3) the stresses resulting from shrinkage are transferred by the interconnections between the fibers (Li et al. 2006). The increase in drying shrinkage values as a result of the increase in basalt fiber can be explained by the fact that the fibers increase the internal friction and make it difficult to settle in the mold. It is estimated that the drying shrinkage values increase as the porosity of the mixtures increases.

Drying shrinkage in mixtures produced from copper slag used instead of fine aggregate showed similar properties to the control mixture. It was even observed that some mixtures containing copper slag show less shrinkage than the control mixture (Hwang and Laiw 1989; Shoya et al. 1997). In the study conducted by Gupta et al., copper slag used instead of aggregate increased the shrinkage values of concretes (Gupta et al. 2017). In the study by You et al., using 60% copper slag instead of aggregate increased the drying shrinkage values (You et al. 2020). In addition, in some studies, if copper slag is used at a high rate, segregation and bleeding occur and drying shrinkage increase (Zhang et al. 2015; Han and Wang 2016; Mastali et al. 2018). In the study conducted by Sharifi et al., copper slag used instead of coarse aggregate up

to 100% reduced the drying shrinkage. This positive effect can be explained by the high adherence of copper aggregate to cement paste (Sharifi et al. 2020). There is no study in the literature that deals with the drying shrinkage behavior of copper slag by using it instead of cement. Therefore, a comment was made on the effect of paste volume on drying shrinkage. Because there are studies in the literature showing that drying shrinkage is directly related to the paste volume. Drying shrinkage may increase as a result of the increase in paste volume (Bissonnette et al. 1999; Rozière et al. 2007).

3.5. Sulphate Resistance Properties of Cement Based Composites

The behavior of the mixtures produced from 6 mm long fibers under the effect of 5% sodium sulphate is given in Fig. 22. After the mixtures numbered 1,4,5,6 and 7 were put into sodium sulphate solution, there was a slight decrease in their size. These mixtures have shown an expansion feature mostly from the 14th day. It is seen that the mixture number 1 with a W/B ratio of 0.40 and without copper slag and copper aggregate shows the least expansion. However, the occurrence of shrinkage for the first 14 days in this effect was an important situation. The expansion values of the other mixtures (4 and 7) with a W/B ratio of 0.40 were also relatively low. The expansion value of the 6th mixture with a W/B ratio of 0.60 and fiber ratio of 2% was found to be $759x10^{-6}$. The reason for the low expansion despite the high w/b ratio is the 15% copper slag used in its content. It was stated in the studies that the C_3A content in the cement structure affects the sulphate resistance. As the C_3A content in cements decreases, sulphate resistance increases (Kaplan and Öztürk 2019). The highest expansion value was obtained in the mixture numbered 9 as approximately $2500x10^{-6}$. Mixture numbered 9 has a w/b ratio of 0.60 and is produced with 50% copper aggregate. Since copper aggregate decreases the total aggregate volume, the porosity of the mixture increased, as a result, also the expansion values increased. The expansion values of mixtures numbered 6 and 8 using 15% copper slag were determined as approximately $1000x10^{-6}$. The use of copper slag made an important contribution to sulphate resistance. A significant effect of the fiber ratio on sulphate resistance was not determined. In Fig. 23, time-dependent sulphate resistance of the mixtures produced from 12 mm long fibers is given

As seen in Fig. 23, mixtures numbered 10, 11 and 12 showed similar properties. It is seen that the mixture numbered 12 with a ratio of 0.60 w/b has an expansion value of approximately $1500x10^{-6}$. It was observed that the 7.5% copper slag used in the mixture numbered 12 contributed positively to this process. It is seen that the mixtures numbered 13, 15, 16,17 and 18 exceed the expansion value of $2000x10^{-6}$. The w/b value of the mixture numbered 15 is 0.60 and no copper slag is used instead of cement. The fiber ratio of 2% in the mixture is not very effective in preventing sulphate expansion. Although the w/b ratio of the mixture number 16 is 0.40 and the copper slag is 15%, it is seen that a relatively high expansion occurs in its structure. This is thought to occur with increased porosity as a result of reduction in aggregate and paste volume with 25% copper aggregate and 15% copper slag. It is seen that the mixture numbered 18 shows a high expansion due to the w/b ratio of 0.60.

As a result of the increase in fiber length, the sulphate-based expansion values of the mixtures also increased. In addition, it was determined that the mixtures numbered 1, 4, 7 and 11 with high compressive strength (> 60 MPa) had less expansion than other mixtures. More expansions occurred in mixtures numbered 9, 17 and 18 with low compressive strength (< 40 MPa). The reason for the high sulfate expansion value of the mixture numbered 9 was explained by the high depth of water penetration (~ 1.5 mm). It was observed that the mixture numbered 6 with a high water penetration depth (~ 1.8 mm) did not cause excess sulphate expansion. This is due to the 15% copper slag used instead of cement. This situation is also reflected in sulphate expansion, since the water penetration depth of the mixture numbered 18 is approximately 1.60 mm.

There is little information in the literature about the contribution of basalt fiber to chemical durability. In the study conducted by Hanafi, the use of basalt fiber reduced the expansions caused by sodium sulfate (Hanafi et al. 2020). Myadaraboina et al. stated in their study that chloride and sulphates do not directly damage basalt fiber (Myadaraboina et al. 2014). There are many studies in the literature indicating that the durability properties of cement-based composites are improved by using fibers (Brandt 2008; Karahan and Atiş 2011; Yehia et al. 2016).

Toshiki et al evaluated copper slag as fine aggregate. As a result of the study, it was observed that copper slag improved the durability properties of concrete (Ayano et al. 2000). When copper slag is used instead of aggregate, the carbonation rate decreased as well as the increase in sulphate resistance (Hwang and Laiw 1989).

Partial replacement of industrial wastes such as slag, fly ash and silica fume instead of cement is known to be a useful technique to increase the durability of concrete to sulphate attack (Freeman and Carrasquillo 1991; Al-Dulaijan et al. 2003). In the study conducted by Onuaguluchi and Eren, copper slag used instead of cement increased the expansion values due to sulphate. This negative property of copper slag was explained by the permeability. This was observed since the permeability of the mixtures increases as the copper slag ratio increases (Onuaguluchi and Eren 2012).

3.6. Freeze-Thaw Resistance of Cement Based Composites

Fig. 24 shows the effect of basalt fiber properties and copper wastes on the freeze-thaw resistance. It was determined that 50 F-T cycles do not decrease the flexural strength much (Fig. 24a). Especially in mixtures with a w/b ratio of 0.40, a slight increase in flexural strength was observed. This situation may be caused by the incomplete hydration due to impermeability at low w/b ratios. The water leaking from the cracks formed in the mortar with the F-T effect enables the non-hydrated cement grains to participate in hydration. As a result, strength increase was observed in low F-T cycles. When using 2% of 6 mm long fibers, the flexural strength is generally reduced. However, if the fiber ratio is 3%, the loss of flexural strength after the F-T cycle may decrease. Increasing the fiber length decreases the flexural strength after F-T cycles. As the fiber ratio increases in the mixtures produced from 12 mm long fibers, the flexural strength decreases. The flexural strength after 50 F-T cycles varies between 7.1-8.8 MPa, while the flexural strength after 200 F-T cycles varies between 7.0-6.1 MPa. For the F-T effect, it is more appropriate to use 1% or 3% of 6 mm long fibers.

As seen in Fig. 24b, as the number of F-T cycles increases, the flexural strength of the mixtures decreases. After 50 F-T cycles, the flexural strength decreased as the copper aggregate increased in mixtures without copper slag. However, with the increase of copper slag, the use of copper aggregate relatively increased the flexural strength. This situation was also observed in mixtures 100 and 200 F-T cycles applied. After 50 F-T cycles, the greatest flexural strength was observed in mixtures using 7.5% copper slag and 50% copper aggregate. After 100 F-T cycles, the use of 15% copper slag and 25% copper aggregate reduced the losses in flexural strength. A similar situation is observed with the 200 F-T effect. Using copper slag in combination with copper aggregate reduced the flexural strength losses resulting from the F-T cycle.

In Fig. 25, it is observed that after all F-T cycles, the flexural strength decreases as the w/b ratio increases. As a result of the 100 and 200 F-T cycles, the flexural strength of the mixtures showed similar properties and fell below 7 MPa. It is observed that mixtures with a ratio of 0.40 W/B are not affected much by F-T cycles. This is related to the fact that the mixtures become more impermeable as a result of the decrease in the w/b ratio.

In Fig. 26, the effect of fiber properties and copper wastes on compressive strength after F-T cycles is given. After 50 F-T cycles, as the ratio of both 6 mm and 12 mm long fibers increased, the compressive strength of the mixtures increased (Fig. 26a). However, the increase in fiber length caused a slight decrease in compressive strength. Especially, the compressive strength of the mixtures obtained from 6 mm long fibers after 50 F-T cycles was over 50 MPa. As the fiber ratio increases in the mixtures obtained from 12 mm long fibers after 100 F-T cycles, the compressive strength increases. For 6 mm long fibers, it was observed that the optimum ratio was 1% or 3%. The compressive strength of all mixtures fell below 50 MPa after 200 F-T. However, the strength loss of the mixtures produced from 6 mm long fibers was less.

As with the flexural strength, the combination of copper aggregate and copper slag has a more positive effect on compressive strength after F-T cycles (Fig. 26b). Using 7.5% of copper slag after 50 F-T cycles increased the compressive strength. However, the compressive strength of the mixtures using copper aggregate was relatively lower. In the case of using 15% copper slag after 100 F-T cycles, the increase in copper aggregate affected positively the compressive strength.

A similar situation was observed after 200 F-T cycles. If the copper slag is 7.5%, 50% copper aggregate generally reduces the strength losses after the F-T cycle.

Figure 27 shows the effect of w/b ratio on compressive strength after F-T cycles. As in the flexural strength, the freeze-thaw resistance of the mixtures decreases as the w/b ratio increases. It is seen that mixtures with a ratio of 0.40 w/b have a compressive strength over 50 MPa even after 200 F-T cycles. A slight increase in compressive strength was observed after 50 F-T cycles of mixtures with a W/B ratio of 0.40.

Using 2% of 6 mm long fibers generally reduces the compressive and flexural strengths after the F-T cycle. One of the reasons for this situation is that the 28-day compressive strengths of these mixtures are generally low (< 40 MPa). It is more appropriate to use 6 mm long fibers in obtaining the mixtures. The combination of copper slag and copper aggregate provided positive results for the F-T effect. The case, that if the copper slag is 7.5%, the copper aggregate is 50%, and if the copper slag is 15%, the copper aggregate is 25%, can improve the mechanical properties after the F-T cycle. It was observed that mixtures with low water penetration depth are usually cases where copper slag and aggregate are used in combination. It is more appropriate to have a w/b ratio of 0.40 for mixtures with this feature.

Researches showed that freezing-thaw resistance can be increased as a result of adding fiber to concrete. In addition, fibers can increase Matrix strength by preventing crack formation and development. The addition of fibers can increase the number of harmless pores, which can reduce the expansion pressure caused by the freezing event, and therefore reduce the degree of damage caused by freezing-thaw (Tiberti et al. 2014; Nam et al. 2016; Zhang et al. 2016). In some studies, the freezing-thaw resistance of concrete was increased by using basalt fiber (Jin et al. 2014; Zhao et al. 2018).

In the study cınducted by Shoya et al., it was reported that the freezing-thaw resistance of concrete is lower than control mixtures if copper slag is used instead of aggregate (Shoya et al. 1997). Ayano and Sakata stated that the freezing-thaw resistance of concrete increases if copper slag is used instead of aggregate (Ayano and Sakata 2000). However, there are a limited number of studies in the literature showing the effects of copper slag on freeze-thaw resistance.

Among the samples that 200 F-T cycles are applied, the samples with the highest loss of strength and visual damage are given in Fig. 28.

3.7. Optimization and Verification Tests of Cement Based Composites

For the mixtures produced according to the Taguchi L18 test matrix, optimization was carried out under three main headings. Optimization groups are presented below.

Group 1: Mechanical Properties

Group 2: Freeze-thaw resistance

Group 3: Dimensional stability and impermeability

For the mechanical properties in the first group, optimization was performed to maximize the compressive and flexural strengths of 7, 28 and 91 days. For the freeze-thaw resistance in group 2, optimization was performed to maximize the mechanical properties (compressive and flexural strength) after 50, 100 and 200 F-T cycles. In the third group, the optimum mixture was found to minimize the sodium sulphate-induced expansion, shrinkage after drying and water penetration depth. Experimental verification was carried out after the estimated properties of the optimum mixes were found. In groups 1 and 2, the target function was chosen as maximize, while in group 3, target function was determined as minimize. Estimated and experimental results of the 1st group are given in Table 7.

Table 7 Optimum mixture ratios for mechanical properties and results of verification tests

Optimum mixing ratios				
Fiber length (mm)	Fiber ratio (%)	Copper slag (%)	Copper aggregate (%)	W/B
6	1	0	0	0.40
Predicted and experimental results				
7 Day-Flexural strength (MPa)-Pre.		7 Day-Flexural strength (MPa)-Exp.		Diff. (%)
6.71		7.21		7.45
28 Day-Flexural strength (MPa)-Pre.		28 Day-Flexural strength (MPa)- Exp.		Diff. (%)
9.93		9.05		8.86
91 Day-Flexural strength (MPa)-Pre.		91 Day-Flexural strength (MPa)- Exp.		Diff. (%)
12.12		10.97		9.49
7 Day-Compressive strength (MPa)-Pre.		7 Day-Compressive strength (MPa)- Exp.		Diff. (%)
67.19		63.46		5.55
28 Day-Compressive strength (MPa)-Pre.		28 Day-Compressive strength (MPa)- Exp.		Diff. (%)
72.39		69.62		3.83
91 Day-Compressive strength (MPa)-Pre.		91 Day-Compressive strength (MPa)- Exp.		Diff. (%)
95.53		89.04		6.79

As seen in Table 7, it may be more appropriate not to use copper wastes when the mechanical properties are desired to be maximum. It was observed that the difference between the estimated and experimental results is less than 10% and there is less deviation percentage in the estimation of compressive strength. Using 1% of the 6 mm long fiber affected the mechanical properties positively.

Table 8 shows the results of optimization for the maximum compressive strength of mixtures as a result of 50, 100 and 200 F-T cycles.

Table 8
Optimum mixture ratios for Freeze-Thaw resistance and results of verification tests

Optimum mixing ratios				
Fiber length (mm)	Fiber ratio (%)	Copper slag(%)	Copper aggregate (%)	W/B
6	3	7.5	0	0.40
Predicted and experimental results				
After 50 F-T Compressive Strength (MPa)-Pre.		After 50 F-T Compressive Strength (MPa)-Exp.		Diff. (%)
69.39		71.87		3.57
After 100 F-T Compressive Strength (MPa)-Pre.		After 100 F-T Compressive Strength (MPa)-Exp.		Diff. (%)
61.75		64.04		3.71
After 200 F-T Compressive Strength (MPa)-Pre.		After 200 F-T Compressive Strength (MPa)-Exp.		Diff. (%)
56.11		52.82		5.86

In optimization for the freeze-thaw effect, it is more appropriate to use 3% of 6 mm long fiber. The degree of damage was reduced by controlling the stresses caused by the freezing effect with increasing fiber content. In addition, the use of copper slag at the rate of 7.5% also made a positive contribution to the freeze-thaw resistance. After 200 F-T cycles, it was observed that it is possible to obtain mixtures with compressive strength over 50 MPa by using a low percentage of copper slag. It was also observed that the w/b ratio of the mixture of 0.40 has a significant effect in reducing the damage after 200 F-T cycles. Low w/b ratio and high fiber content were the factors that decreased freeze-thaw damage.

In Table 9, the required mixture ratios are given to minimize the depth of water penetration, drying shrinkage and sodium sulphate-induced expansion.

Table 9
Optimum mixture ratios for impermeability and dimensional stability and results of verification tests

Optimum mixing ratios				
Fiber length (mm)	Fiber ratio (%)	Copper slag(%)	Copper aggregate (%)	W/B
6	1	15	0	0.40
Predicted and experimental results				
Water penetration depth (mm)-Pre.		Water penetration depth (mm)-Exp.		Diff. (%)
0.93		1.01		8.60
Drying shrinkage (10^{-6})-Pre.		Drying shrinkage (10^{-6})-Exp.		Diff. (%)
1195		1307		9.37
Sulphate expansion (10^{-6})-Pre.		Sulphate expansion (10^{-6})-Exp.		Diff. (%)
365		401		9.86

As seen in Table 9, the fact that copper slag is 15% contributes to the dimensional stability of the mixtures. It was particularly effective in reducing the sodium sulphate-induced expansions. Copper slag used instead of cement contributed to sulphate resistance as it reduced C_3A and CH content. As a result of the increase in copper slag, it can be said that the depth of water penetration increases and accordingly the freeze-thaw resistance increases. The increase in copper aggregate content did not contribute to dimensional stability. Because it has a higher specific weight compared to

crushed stone aggregate, increasing the amount of aggregate decreases the aggregate volume. As a result, the mixture becomes more porous and the shrinkage values may increase. The aggregate volume has an important role in reducing drying shrinkage.

In some studies, it was stated that basalt fiber causes coagulation in concrete and mortar (Meng et al. 2016; Alnahhal and Aljidda 2018). The coagulation of basalt fiber was determined by SEM images by Yan et al. and it was determined that this effect also affects the mechanical properties (Yan et al. 2017). Similar results was observed for shotcrete (Yan et al. 2020). In this study, it is thought that coagulation formed in basalt fiber causes variation in mechanical properties. The variation that occurs with the increase in fiber content may be due to the tendency to coagulation.

Conclusions And Recommendations

As the length and ratio of the fiber used in the mixtures increased, the amount of plasticizer increased. Similar results are valid for the content of copper aggregate and slag. The increase in copper waste increased the amount of plasticizer. Since the increase in fiber content or length increases the internal friction, the amount of plasticizer was increased in order to obtain sufficient workability. The structure of copper aggregate with sharper corners compared to crushed stone aggregate decreased the workability. However, in case of using copper slag and aggregate, attention should be paid to the use of plasticizer. Partial decomposition was observed depending on the amount of plasticizer in the mixture numbered 13 using 7.5% copper slag and 50% copper aggregate. As the W/B ratio increased, the amount of plasticizer was decreased.

While fiber length was not very effective on unit weight of mixtures, increasing fiber ratio decreased unit weight values. Although the workability of the mixtures are close to each other, a more hollow structure was formed with the increase in the fiber ratio while placing into the mold. The increase in the ratio of copper slag and copper aggregate increased the unit weight values of the mixtures. The fact that copper waste has a higher specific weight than cement and crushed stone affected this situation. With the increase in the W/B ratio, the unit weight values of the mixtures decreased.

Increasing fiber length generally increased flow diameter. However, this effect occurred because more plasticizer was used in mixtures produced with 12 mm long fibers. A similar result was observed in fiber ratio. The flow diameter of the mixtures with 2% and 3% fiber ratio increased slightly. In the case of copper slag being 7.5%, the flow diameter increased, while in the use of copper slag by 15%, the flow diameter was the same as slag-free mixtures.The use of copper aggregate in the mixtures increased the flow diameter of the mixtures. However, it was determined that 25% and 50% copper aggregates have similar properties in terms of flow diameters.

In terms of mechanical properties (7-28-91 days / Compressive and flexural strength), it is more appropriate to use 1% of 6 mm long fiber. It is more appropriate not to use copper waste in optimization for mechanical properties. However, this situation was observed since the mixtures are prepared according to the material proportions instead of $1m^3$ content. It may not be correct to use such an exact statement for copper waste, as copper aggregate and slag reduce the aggregate and paste volume. To obtain high strength, the w/b ratio should be 0.40.

For the mechanical properties after the F-T cycle, it is appropriate to use 6 mm long fiber. However, the fiber ratio being 3% copper slag ratio 7.5% contributes positively to the freeze-thaw resistance. A w/b ratio of 0.40 for impermeability reduces the strength loss. In terms of freeze-thaw resistance, it is appropriate to have a copper aggregate ratio of 0%.

In terms of sorptivity and dimensional stability, the use of 1% fiber of 6 mm length provided more positive results. The use of 15% copper slag made an important contribution in reducing the sulphate expansion. The very positive feature of the use of copper aggregate to reduce drying shrinkage could not be obtained. Because as the rate of copper aggregate increases, the aggregate volume decreases. In addition, the use of 7.5% copper slag reduces the water penetration depth of the mixtures.

In general, it is more useful to use 1% of 6 mm long fiber in mixtures. Being 0.40 of the w/b ratio of the mixtures is important in terms of strength and durability. While the use of copper aggregate does not provide improvement in strength and durability properties, the use of copper slag at a rate of 7.5% reduces the depth of water penetration and 15% reduces the sulphate expansion. However, it is possible to obtain a more environmentally friendly composite by sacrificing the strength and durability properties of the mixtures. For example, in mixtures using 15% copper slag and 50% copper aggregate, a 28-day compressive strength of approximately 52 MPa was achieved. If the copper aggregate is 25%, its strength and durability properties may deteriorate a little, but a more environmentally useful mixture can be obtained.

As a result, copper slag and aggregate were not found to have a very positive effect on mechanical properties, but it was observed that copper slag is more effective in terms of durability. It was determined that copper aggregate can also be used by using up to 25%, and by sacrificing some concrete properties. In this way, waste, which is an environmental problem, will be disposed of.

It was observed that it is possible to directly use the copper wastes generated in the field in traditional concrete and shotcrete used in tunnels and drifts in copper mines.

By using copper slag together with pozzolanes such as fly ash and silica fume, its effect on the properties of cement-based composites can be examined. In addition, since the specific gravity of copper aggregate is high, it may be appropriate to use in heavyweight concrete design. Examining the freeze-thaw and sulphate resistance of composites produced with basalt fiber in a longer period will contribute to the literature. In addition, it may be more appropriate to use copper waste in geopolymer design.

Declarations

Compliance with ethical standards

Competing interest: The authors declare that they have no competing interests.

Ethics approval and consent to participate: Not applicable

Consent for publication: Not applicable

Funding: Not applicable

Authors' contributions: Gokhan Kaplan; Contributed to the writing of the article and the literature review. Mohammed Najı Ahmed Abu Aeshah; Perofrmed the experiments and analyse the results.

Availability of data and materials: Data and material are not available for research purpose and for reference.

References

1. Adesina A, Bastani A, Heydariha JZ et al (2020) Performance of basalt fibre-reinforced concrete for pavement and flooring applications. Innov Infrastruct Solut 5:103. https://doi.org/10.1007/s41062-020-00359-y
2. Ahmad MR, Chen B, Yu J (2019) A comprehensive study of basalt fiber reinforced magnesium phosphate cement incorporating ultrafine fly ash. Composites Part B: Engineering 168:204–217. https://doi.org/10.1016/j.compositesb.2018.12.065
3. Al-Dulaijan SU, Maslehuddin M, Al-Zahrani MM et al (2003) Sulfate resistance of plain and blended cements exposed to varying concentrations of sodium sulfate. Cem Concr Compos 25:429–437. https://doi.org/10.1016/S0958-9465(02)00083-5

4. Algin Z, Ozen M (2018) The properties of chopped basalt fibre reinforced self-compacting concrete. Constr Build Mater. https://doi.org/10.1016/j.conbuildmat.2018.07.089
5. Al-Jabri KS, Al-Saidy AH, Taha R (2011) Effect of copper slag as a fine aggregate on the properties of cement mortars and concrete. Constr Build Mater 25:933–938. https://doi.org/10.1016/j.conbuildmat.2010.06.090
6. Al-Jabri KS, Hisada M, Al-Oraimi SK, Al-Saidy AH (2009) Copper slag as sand replacement for high performance concrete. Cem Concr Compos 31:483–488. https://doi.org/10.1016/j.cemconcomp.2009.04.007
7. Al-Jabri KS, Taha RA, Al-Hashmi A, Al-Harthy AS (2006) Effect of copper slag and cement by-pass dust addition on mechanical properties of concrete. Constr Build Mater. https://doi.org/10.1016/j.conbuildmat.2005.01.020
8. Al-Masoodi AHH, Kawan A, Kasmuri M et al (2016) Static and dynamic properties of concrete with different types and shapes of fibrous reinforcement. Constr Build Mater 104:247–262. https://doi.org/10.1016/j.conbuildmat.2015.12.037
9. Alnahhal W, Aljidda O (2018) Flexural behavior of basalt fiber reinforced concrete beams with recycled concrete coarse aggregates. Constr Build Mater. https://doi.org/10.1016/j.conbuildmat.2018.02.135
10. Ambily PS, Umarani C, Ravisankar K et al (2015) Studies on ultra high performance concrete incorporating copper slag as fine aggregate. Constr Build Mater. https://doi.org/10.1016/j.conbuildmat.2014.12.092
11. Ariño AM, Mobasher B (1999) Effect of ground copper slag on strength and toughness of cementitious mixes. ACI Mater J. https://doi.org/10.14359/430
12. Asprone D, Cadoni E, Iucolano F, Prota A (2014) Analysis of the strain-rate behavior of a basalt fiber reinforced natural hydraulic mortar. Cem Concr Compos. https://doi.org/10.1016/j.cemconcomp.2014.06.009
13. ASTM C348 (2021) Test Method for Flexural Strength of Hydraulic-Cement Mortars
14. ASTM C349 (2018) Test Method for Compressive Strength of Hydraulic-Cement Mortars. Using Portions of Prisms Broken in Flexure
15. ASTM C596 (2018) Test Method for Drying. Shrinkage of Mortar Containing Hydraulic Cement
16. ASTM C666 (2003) Test Method for Resistance of Concrete to Rapid Freezing and Thawing
17. ASTM C1012 (2018) Test Method for Length Change of Hydraulic-Cement Mortars Exposed to a Sulfate Solution
18. ASTM C1437 (2020) Standard Test Method for Flow of Hydraulic Cement Mortar
19. ASTM C1585 (2020) Test Method for Measurement of Rate. of Absorption of Water by Hydraulic-Cement Concretes
20. Ayano T, Kuramoto O, Sakata K (2000) Concrete with Copper Slag Fine Aggregate. Journal of the Society of Materials Science Japan 49:1097–1102. https://doi.org/10.2472/jsms.49.1097
21. Ayano T, Sakata K (2000) Durability of Concrete with Copper Slag Fine Aggregate. Special Publication 192:141–158. https://doi.org/10.14359/5746
22. Bayraktar OY (2021) Possibilities of disposing silica fume and waste glass powder, which are environmental wastes, by using as a substitute for Portland cement. Environ Sci Pollut Res 28:16843–16854. https://doi.org/10.1007/s11356-020-12195-9
23. Bissonnette B, Pierre P, Pigeon M (1999) Influence of key parameters on drying shrinkage of cementitious materials. Cem Concr Res 29:1655–1662. https://doi.org/10.1016/S0008-8846(99)00156-8
24. Borhan TM (2012) Properties of glass concrete reinforced with short basalt fibre. Materials Design 42:265–271. https://doi.org/10.1016/j.matdes.2012.05.062
25. Brandt AM (2008) Fibre reinforced cement-based (FRC) composites after over 40 years of development in building and civil engineering. Compos Struct 86:3–9. https://doi.org/10.1016/j.compstruct.2008.03.006
26. Branston J, Das S, Kenno SY, Taylor C (2016) Mechanical behaviour of basalt fibre reinforced concrete. Constr Build Mater. https://doi.org/10.1016/j.conbuildmat.2016.08.009

27. Chen B, Liu J (2005) Contribution of hybrid fibers on the properties of the high-strength lightweight concrete having good workability. Cem Concr Res 35:913–917. https://doi.org/10.1016/j.cemconres.2004.07.035
28. Chen JJ, Kwan AKH, Jiang Y (2014) Adding limestone fines as cement paste replacement to reduce water permeability and sorptivity of concrete. Constr Build Mater 56:87–93. https://doi.org/10.1016/j.conbuildmat.2014.01.066
29. Chidighikaobi PC (2019) Thermal effect on the flexural strength of expanded clay lightweight basalt fiber reinforced concrete. Materials Today: Proceedings 19:2467–2470. https://doi.org/10.1016/j.matpr.2019.08.110
30. Chithra S, Senthil Kumar SRR, Chinnaraju K (2016) The effect of Colloidal Nano-silica on workability, mechanical and durability properties of High Performance Concrete with Copper slag as partial fine aggregate. Constr Build Mater 113:794–804. https://doi.org/10.1016/j.conbuildmat.2016.03.119
31. Chu SH (2019) Effect of paste volume on fresh and hardened properties of concrete. Constr Build Mater 218:284–294. https://doi.org/10.1016/j.conbuildmat.2019.05.131
32. Corinaldesi V, Nardinocchi A (2016) Influence of type of fibers on the properties of high performance cement-based composites. Constr Build Mater 107:321–331. https://doi.org/10.1016/j.conbuildmat.2016.01.024
33. Davis R, John P (2018) Application of Taguchi-Based Design of Experiments for Industrial Chemical Processes. In: Silva V (ed) Statistical Approaches With Emphasis on Design of Experiments Applied to Chemical Processes. InTech
34. Deák T, Czigány T (2009) Chemical Composition and Mechanical Properties of Basalt and Glass Fibers: A Comparison. Text Res J. https://doi.org/10.1177/0040517508095597
35. Dhand V, Mittal G, Rhee KY et al (2015) A short review on basalt fiber reinforced polymer composites. Composites Part B: Engineering 73:166–180. https://doi.org/10.1016/j.compositesb.2014.12.011
36. Dias DP, Thaumaturgo C (2005) Fracture toughness of geopolymeric concretes reinforced with basalt fibers. Cem Concr Compos 27:49–54. https://doi.org/10.1016/j.cemconcomp.2004.02.044
37. dos Anjos MAG, Sales ATC, Andrade N (2017) Blasted copper slag as fine aggregate in Portland cement concrete. J Environ Manage 196:607–613. https://doi.org/10.1016/j.jenvman.2017.03.032
38. Edwin RS, De Schepper M, Gruyaert E, De Belie N (2016) Effect of secondary copper slag as cementitious material in ultra-high performance mortar. Constr Build Mater. https://doi.org/10.1016/j.conbuildmat.2016.05.007
39. Elshafie S, Whittleston G, A REVIEW OF THE EFFECT OF BASALT FIBRE LENGTHS AND PROPORTIONS ON THE MECHANICAL PROPERTIES OF CONCRETE
40. Emdadi A, Mehdipour I, Libre NA, Shekarchi M (2015) Optimized workability and mechanical properties of FRCM by using fiber factor approach: theoretical and experimental study. Mater Struct 48:1149–1161. https://doi.org/10.1617/s11527-013-0221-3
41. EN 197-1 (2002) Cement- Part 1:. Compositions and conformity criteria for common cements
42. Esmaeili J, Aslani H (2019) Use of copper mine tailing in concrete: strength characteristics and durability performance. J Mater Cycles Waste Manag 21:729–741. https://doi.org/10.1007/s10163-019-00831-7
43. Fallah S, Nematzadeh M (2017) Mechanical properties and durability of high-strength concrete containing macro-polymeric and polypropylene fibers with nano-silica and silica fume. Constr Build Mater 132:170–187. https://doi.org/10.1016/j.conbuildmat.2016.11.100
44. Fantous T, Yahia A (2020) Effect of viscosity and shear regime on stability of the air-void system in self-consolidating concrete using Taguchi method. Cem Concr Compos 112:103653. https://doi.org/10.1016/j.cemconcomp.2020.103653
45. Fiore V, Scalici T, Di Bella G, Valenza A (2015) A review on basalt fibre and its composites. Composites Part B: Engineering 74:74–94. https://doi.org/10.1016/j.compositesb.2014.12.034
46. Freedoniagroup (2016) World Construction Aggregates

47. Freeman RB, Carrasquillo RL (1991) Influence of the method of fly ash incorporation on the sulfate resistance of fly ash concrete. Cem Concr Compos 13:209–217. https://doi.org/10.1016/0958-9465(91)90022-A
48. Geetha S, Madhavan S (2017) High Performance Concrete with Copper slag for Marine Environment. Materials Today: Proceedings 4:3525–3533. https://doi.org/10.1016/j.matpr.2017.02.243
49. Ghazy A, Bassuoni MT, Maguire E, O'Loan M (2016) Properties of Fiber-Reinforced Mortars Incorporating Nano-Silica. Fibers 4:6. https://doi.org/10.3390/fib4010006
50. Gupta N, Siddique R (2020) Durability characteristics of self-compacting concrete made with copper slag. Constr Build Mater 247:118580. https://doi.org/10.1016/j.conbuildmat.2020.118580
51. Gupta RC, Mehra P, Thomas BS (2017) Utilization of Copper Tailing in Developing Sustainable and Durable Concrete. J Mater Civ Eng 29:04016274. https://doi.org/10.1061/(ASCE)MT.1943-5533.0001813
52. Hagelüken C (2006) Recycling of Electronic Scrap at Umicore. Precious Metals Refining
53. Han J, Wang K (2016) Influence of bleeding on properties and microstructure of fresh and hydrated Portland cement paste. Constr Build Mater 115:240–246. https://doi.org/10.1016/j.conbuildmat.2016.04.059
54. Hanafi M, Aydin E, Ekinci A (2020) Engineering Properties of Basalt Fiber-Reinforced Bottom Ash Cement Paste Composites. Materials 13:1952. https://doi.org/10.3390/ma13081952
55. Hasan A, Maroof N, Ibrahim Y (2019) Effects of Polypropylene Fiber Content on Strength and Workability Properties of Concrete. Polytechnic j 9:7–12. https://doi.org/10.25156/ptj.v9n1y2019.pp7-12
56. Hashem FS, Amin MS, Hekal EE (2011) Stabilization of Cu (II) wastes by C3S hydrated matrix. Constr Build Mater 25:3278–3282. https://doi.org/10.1016/j.conbuildmat.2011.03.015
57. High C, Seliem HM, El-Safty A, Rizkalla SH (2015) Use of basalt fibers for concrete structures. Constr Build Mater. https://doi.org/10.1016/j.conbuildmat.2015.07.138
58. Hong LT, Lubell AS (2015) Phosphate Cement-Based Concretes Containing Silica Fume. MJ 112:587–596. https://doi.org/10.14359/51687178
59. Hwang C-L, Laiw J-C (1989) Properties of Concrete Using Copper Slag. as a Substitute for Fine Aggregate
60. International Copper Study Group (2016) The World Copper Factbook
61. Irine IAF (2014) Strength Aspects of Basalt Fiber Reinforced Concrete
62. Ishimaru K, Mizuguchi H, Hashimoto C et al (2005) Properties of Concrete Using Copper Slag and Second Class Fly Ash as a Part of Fine Aggregate. Journal of the Society of Materials Science Japan 54:828–833. https://doi.org/10.2472/jsms.54.828
63. Jalasutram S, Sahoo DR, Matsagar V (2017) Experimental investigation of the mechanical properties of basalt fiber-reinforced concrete. Structural Concrete 18:292–302. https://doi.org/10.1002/suco.201500216
64. Jiang C, Fan K, Wu F, Chen D (2014) Experimental study on the mechanical properties and microstructure of chopped basalt fibre reinforced concrete. Materials Design 58:187–193. https://doi.org/10.1016/j.matdes.2014.01.056
65. Jiang C, Huang S, Zhu Y et al (2016) Effect of Polypropylene and Basalt Fiber on the Behavior of Mortars for Repair Applications. Advances in Materials Science and Engineering 2016:e5927609. https://doi.org/10.1155/2016/5927609
66. Jiang CH, McCarthy TJ, Chen D, Dong QQ (2010) Influence of Basalt Fiber on Performance of Cement Mortar. Key Eng Mater 426–427:93–96. https://doi.org/10.4028/www.scientific.net/KEM.426-427.93
67. Jin SJ, Li ZL, Zhang J, Wang YL (2014) Experimental Study on the Performance of the Basalt Fiber Concrete Resistance to Freezing and Thawing. Appl Mech Mater 584–586:1304–1308. https://doi.org/10.4028/www.scientific.net/AMM.584-586.1304
68. Kabay N (2014) Abrasion resistance and fracture energy of concretes with basalt fiber. Constr Build Mater 50:95–101. https://doi.org/10.1016/j.conbuildmat.2013.09.040

69. Kaplan G, Gulcan A, Cagdas B, Bayraktar OY (2021) The impact of recycled coarse aggregates obtained from waste concretes on lightweight pervious concrete properties. Environ Sci Pollut Res 28:17369–17394. https://doi.org/10.1007/s11356-020-11881-y
70. Kaplan G, Öztürk AU (2019) Dimensional Stability and Microstructural Properties of Cements with Different C3A Contents. INAE Lett 4:15–26. https://doi.org/10.1007/s41403-018-00061-7
71. Kaplan G, Salem Elmekahal MA (2021) Microstructure and durability properties of lightweight and high-performance sustainable cement-based composites with rice husk ash. Environ Sci Pollut Res. https://doi.org/10.1007/s11356-021-14489-y
72. Karahan O, Atiş CD (2011) The durability properties of polypropylene fiber reinforced fly ash concrete. Materials Design 32:1044–1049. https://doi.org/10.1016/j.matdes.2010.07.011
73. Karthikeyan B, Subin A, Muthulakshmi T, HIGH STRENGTH CONCRETE USING ULTRA-FINE TIO2 AND BASALT FIBER-A STUDY ON MECHANICAL AND DURABILITY CHARACTERISTICS. 8
74. Katkhuda H, Shatarat N (2017) Improving the mechanical properties of recycled concrete aggregate using chopped basalt fibers and acid treatment. Constr Build Mater. https://doi.org/10.1016/j.conbuildmat.2017.02.128
75. Khanzadi M, Behnood A (2009) Mechanical properties of high-strength concrete incorporating copper slag as coarse aggregate. Constr Build Mater. https://doi.org/10.1016/j.conbuildmat.2008.12.005
76. Kolias S, Georgiou C (2005) The effect of paste volume and of water content on the strength and water absorption of concrete. Cem Concr Compos 27:211–216. https://doi.org/10.1016/j.cemconcomp.2004.02.009
77. Li W, Xu J (2009) Mechanical properties of basalt fiber reinforced geopolymeric concrete under impact loading. Materials Science Engineering: A 505:178–186. https://doi.org/10.1016/j.msea.2008.11.063
78. Li Y, Shen A, Wu H (2020) Fractal Dimension of Basalt Fiber Reinforced Concrete (BFRC) and Its Correlations to Pore Structure, Strength and Shrinkage. Materials 13:3238. https://doi.org/10.3390/ma13143238
79. Li Z, Perez Lara MA, Bolander JE (2006) Restraining effects of fibers during non-uniform drying of cement composites. Cem Concr Res 36:1643–1652. https://doi.org/10.1016/j.cemconres.2006.04.001
80. Liu H, Li W, Luo G et al (2020) Mechanical properties and fracture behavior of crumb rubber basalt fiber concrete based on acoustic emission technology. Sensors (Switzerland). https://doi.org/10.3390/s20123513
81. Liu J, Guo R, Shi P, Huang L (2019) Hydration mechanisms of composite binders containing copper slag at different temperatures. J Therm Anal Calorim 137:1919–1928. https://doi.org/10.1007/s10973-019-08116-9
82. Mastali M, Kinnunen P, Dalvand A et al (2018) Drying shrinkage in alkali-activated binders – A critical review. Constr Build Mater 190:533–550. https://doi.org/10.1016/j.conbuildmat.2018.09.125
83. Mavroulidou M (2017) Mechanical Properties and Durability of Concrete with Water Cooled Copper Slag Aggregate. Waste, Valorization B. https://doi.org/10.1007/s12649-016-9819-3
84. Meng W, Liu H, Liu G et al (2016) Bond-slip constitutive relation between BFRP bar and basalt fiber recycled-aggregate concrete. KSCE J Civ Eng 20:1996–2006. https://doi.org/10.1007/s12205-015-0350-z
85. Menten T (1991) Quality Engineering Using Robust Design. Technometrics 33:235–236. https://doi.org/10.1080/00401706.1991.10484810
86. Militký J, Kovačič V, Rubnerová J (2002) Influence of thermal treatment on tensile failure of basalt fibers. Eng Fract Mech 69:1025–1033. https://doi.org/10.1016/S0013-7944(01)00119-9
87. Mobasher B, Devaguptapu R, Arino AM (1996) Effect of copper slag on the hydration of blended cementitious mixtures. In: Proceedings of the Materials Engineering Conference
88. Morozov NN, Bakunov VS, Morozov EN et al (2001) Materials Based on Basalts from the European North of Russia. Glass Ceram 58:100–104. https://doi.org/10.1023/A:1010947415202

89. Moura W, Masuero A, Molin D, Dal Vilela A (1999) Concrete performance with admixtures of electrical steel slag and copper slag concerning mechanical properties. American Concrete Institute
90. Moura WA, Gonçalves JP, Lima MBL (2007) Copper slag waste as a supplementary cementing material to concrete. J Mater Sci 42:2226–2230. https://doi.org/10.1007/s10853-006-0997-4
91. Myadaraboina H, Law D, Patnaikuni I (2014) Durability Of Basalt Fibers In Concrete Medium. Proceedings of International Structural Engineering and Construction 1:. https://doi.org/10.14455/ISEC.res.2014.41
92. Nagarajan D, R T, Neelamegam M, Prakash R (2020) Characterization and behavior of basalt fiber-reinforced lightweight concrete. Structural Concrete 22:. https://doi.org/10.1002/suco.201900390
93. Najimi M, Pourkhorshidi AR (2011) Properties of concrete containing copper slag waste. Magazine of Concrete Research. https://doi.org/10.1680/macr.2011.63.8.605
94. Najimi M, Sobhani J, Pourkhorshidi AR (2011) Durability of copper slag contained concrete exposed to sulfate attack. Constr Build Mater. https://doi.org/10.1016/j.conbuildmat.2010.11.067
95. Nam J, Kim G, Lee B et al (2016) Frost resistance of polyvinyl alcohol fiber and polypropylene fiber reinforced cementitious composites under freeze thaw cycling. Composites Part B: Engineering 90:241–250. https://doi.org/10.1016/j.compositesb.2015.12.009
96. Nasir V, Karimipour H, Taheri-Behrooz F, Shokrieh MM (2012) Corrosion behaviour and crack formation mechanism of basalt fibre in sulphuric acid. Corros Sci. https://doi.org/10.1016/j.corsci.2012.06.028
97. Niu D, Su L, Luo Y et al (2020) Experimental study on mechanical properties and durability of basalt fiber reinforced coral aggregate concrete. Constr Build Mater. https://doi.org/10.1016/j.conbuildmat.2019.117628
98. Novitskii AG (2004) High-Temperature Heat-Insulating Materials Based on Fibers from Basalt-Type Rock Materials. Refract Ind Ceram 45:144–146. https://doi.org/10.1023/B:REFR.0000029624.43008.ef
99. Onuaguluchi O, Eren Ö (2013) Rheology, strength and durability properties of mortars containing copper tailings as a cement replacement material. European Journal of Environmental Civil Engineering 17:19–31. https://doi.org/10.1080/19648189.2012.699708
100. Onuaguluchi O, Eren Ö (2012) Durability-related properties of mortar and concrete containing copper tailings as a cement replacement material. Magazine of Concrete Research 64:1015–1023. https://doi.org/10.1680/macr.11.00170
101. Pehlivanlı ZO, Uzun İ, Yücel ZP, Demir İ (2016) The effect of different fiber reinforcement on the thermal and mechanical properties of autoclaved aerated concrete. Constr Build Mater 112:325–330. https://doi.org/10.1016/j.conbuildmat.2016.02.223
102. Prem PR, Verma M, Ambily PS (2018) Sustainable cleaner production of concrete with high volume copper slag. J Clean Prod. https://doi.org/10.1016/j.jclepro.2018.04.245
103. Punurai W, Kroehong W, Saptamongkol A, Chindaprasirt P (2018) Mechanical properties, microstructure and drying shrinkage of hybrid fly ash-basalt fiber geopolymer paste. Constr Build Mater 186:62–70. https://doi.org/10.1016/j.conbuildmat.2018.07.115
104. Qin J, Qian J, Li Z et al (2018) Mechanical properties of basalt fiber reinforced magnesium phosphate cement composites. Constr Build Mater 188:946–955. https://doi.org/10.1016/j.conbuildmat.2018.08.044
105. Quagliarini E, Monni F, Lenci S, Bondioli F (2012) Tensile characterization of basalt fiber rods and ropes: A first contribution. Constr Build Mater 34:372–380. https://doi.org/10.1016/j.conbuildmat.2012.02.080
106. Rajasekar A, Arunachalam K, Kottaisamy M (2019) Assessment of strength and durability characteristics of copper slag incorporated ultra high strength concrete. J Clean Prod 208:402–414. https://doi.org/10.1016/j.jclepro.2018.10.118

107. Ralegaonkar R, Gavali H, Aswath P, Abolmaali S (2018) Application of chopped basalt fibers in reinforced mortar: A review. Constr Build Mater 164:589–602. https://doi.org/10.1016/j.conbuildmat.2017.12.245
108. Ramanathan P, Baskar I, Muthupriya P, Venkatasubramani R (2013) Performance of self-compacting concrete containing different mineral admixtures. KSCE J Civ Eng 17:465–472. https://doi.org/10.1007/s12205-013-1882-8
109. Ranganath RV, Bhattacharjee B, Krishnamoorthy S (1998) Influence of Size Fraction of Ponded Ash on its Pozzolanic Activity. Cem Concr Res 28:749–761. https://doi.org/10.1016/S0008-8846(98)00036-2
110. Rozière E, Granger S, Turcry Ph, Loukili A (2007) Influence of paste volume on shrinkage cracking and fracture properties of self-compacting concrete. Cem Concr Compos 29:626–636. https://doi.org/10.1016/j.cemconcomp.2007.03.010
111. Ruijie M, Yang J, Liu Y, Zheng X (2017) Influence of length-to-diameter ratio on shrinkage of basalt fiber concrete. IOP Conf Ser: Mater Sci Eng 242:012027. https://doi.org/10.1088/1757-899X/242/1/012027
112. Sadrmomtazi A, Tahmouresi B, Saradar A (2018) Effects of silica fume on mechanical strength and microstructure of basalt fiber reinforced cementitious composites (BFRCC). Constr Build Mater 162:321–333. https://doi.org/10.1016/j.conbuildmat.2017.11.159
113. Saloni P, Pham TM (2020) Enhanced properties of high-silica rice husk ash-based geopolymer paste by incorporating basalt fibers. Constr Build Mater 245:118422. https://doi.org/10.1016/j.conbuildmat.2020.118422
114. Sharifi Y, Afshoon I, Asad-Abadi S, Aslani F (2020) Environmental protection by using waste copper slag as a coarse aggregate in self-compacting concrete. J Environ Manage 271:111013. https://doi.org/10.1016/j.jenvman.2020.111013
115. Sharma R, Khan RA (2018) Influence of copper slag and metakaolin on the durability of self compacting concrete. J Clean Prod. https://doi.org/10.1016/j.jclepro.2017.10.029
116. Sharma R, Khan RA (2017a) Sustainable use of copper slag in self compacting concrete containing supplementary cementitious materials. J Clean Prod 151:179–192. https://doi.org/10.1016/j.jclepro.2017.03.031
117. Sharma R, Khan RA (2017b) Durability assessment of self compacting concrete incorporating copper slag as fine aggregates. Constr Build Mater 155:617–629. https://doi.org/10.1016/j.conbuildmat.2017.08.074
118. Shi C, Qian J (2000) High performance cementing materials from industrial slags — a review. Resour Conserv Recycl 29:195–207. https://doi.org/10.1016/S0921-3449(99)00060-9
119. Shirdam R, Amini M, Bakhshi N (2019) Investigating the Effects of Copper Slag and Silica Fume on Durability, Strength, and Workability of Concrete. Int J Environ Res 13:909–924. https://doi.org/10.1007/s41742-019-00215-7
120. Shoya M, Nagataki S, Tomosawa F, Tsukinaga SS and Y (1997) Freezing and Thawing Resistance of Concrete With Excessive Bleeding and Its Improvement. SP 170:879–898. https://doi.org/10.14359/6858
121. Sim J, Park C, Moon DY (2005) Characteristics of basalt fiber as a strengthening material for concrete structures. Composites Part B: Engineering. https://doi.org/10.1016/j.compositesb.2005.02.002
122. Simões T, Costa H, Dias-da-Costa D, Júlio E (2017) Influence of fibres on the mechanical behaviour of fibre reinforced concrete matrixes. Constr Build Mater 137:548–556. https://doi.org/10.1016/j.conbuildmat.2017.01.104
123. Sun X, Gao Z, Cao P, Zhou C (2019) Mechanical properties tests and multiscale numerical simulations for basalt fiber reinforced concrete. Constr Build Mater 202:58–72. https://doi.org/10.1016/j.conbuildmat.2019.01.018
124. Tassew ST, Lubell AS (2014) Mechanical properties of glass fiber reinforced ceramic concrete. Constr Build Mater 51:215–224. https://doi.org/10.1016/j.conbuildmat.2013.10.046
125. Thomas BS, Damare A, Gupta RC (2013) Strength and durability characteristics of copper tailing concrete. Constr Build Mater. https://doi.org/10.1016/j.conbuildmat.2013.07.075
126. Tiberti G, Minelli F, Plizzari GA, Vecchio FJ (2014) Influence of concrete strength on crack development in SFRC members. Cem Concr Compos 45:176–185. https://doi.org/10.1016/j.cemconcomp.2013.10.004

127. Tixier R, Devaguptapu R, Mobasher B (1997) The effect of copper slag on the hydration and mechanical properties of cementitious mixtures. Cem Concr Res 27:1569–1580. https://doi.org/10.1016/S0008-8846(97)00166-X
128. Toklu K, Şimşek O (2018) Investigation of mechanical properties of repair mortars containing high-volume fly ash and nano materials. J Aust Ceram Soc 54:261–270. https://doi.org/10.1007/s41779-017-0150-7
129. Tumadhir M, Borhan (2013) Thermal and Mechanical Properties of Basalt Fibre Reinforced Concrete. International Journal of Civil and Environmental Engineering
130. Wu G, Wang X, Wu Z et al (2015) Durability of basalt fibers and composites in corrosive environments. J Compos Mater. https://doi.org/10.1177/0021998314526628
131. Wu W, Zhang W, Ma G (2010a) Optimum content of copper slag as a fine aggregate in high strength concrete. Materials Design 31:2878–2883. https://doi.org/10.1016/j.matdes.2009.12.037
132. Wu W, Zhang W, Ma G (2010b) Mechanical properties of copper slag reinforced concrete under dynamic compression. Constr Build Mater 24:910–917. https://doi.org/10.1016/j.conbuildmat.2009.12.001
133. Yan S, Jiao H, Yang X et al (2020) Bending Properties of Short-Cut Basalt Fiber Shotcrete in Deep Soft Rock Roadway. Advances in Civil Engineering 2020:1–9. https://doi.org/10.1155/2020/5749685
134. Yan X, Shen H, Yu L, Hamada H (2017) Polypropylene–glass fiber/basalt fiber hybrid composites fabricated by direct fiber feeding injection molding process. J Appl Polym Sci 134:45472. https://doi.org/10.1002/app.45472
135. Yehia S, Douba A, Abdullahi O, Farrag S (2016) Mechanical and durability evaluation of fiber-reinforced self-compacting concrete. Constr Build Mater 121:120–133. https://doi.org/10.1016/j.conbuildmat.2016.05.127
136. You N, Liu Y, Gu D et al (2020) Rheology, shrinkage and pore structure of alkali-activated slag-fly ash mortar incorporating copper slag as fine aggregate. Constr Build Mater 242:118029. https://doi.org/10.1016/j.conbuildmat.2020.118029
137. Zain MFM, Islam MN, Radin SS, Yap SG (2004) Cement-based solidification for the safe disposal of blasted copper slag. Cem Concr Compos. https://doi.org/10.1016/j.cemconcomp.2003.08.002
138. Zhang W, Hama Y, Na SH (2015) Drying shrinkage and microstructure characteristics of mortar incorporating ground granulated blast furnace slag and shrinkage reducing admixture. Constr Build Mater 93:267–277. https://doi.org/10.1016/j.conbuildmat.2015.05.103
139. Zhang W, Zhang N, Zhou Y (2016) Effect of flexural impact on freeze–thaw and deicing salt resistance of steel fiber reinforced concrete. Mater Struct 49:5161–5168. https://doi.org/10.1617/s11527-016-0851-3
140. Zhao Y-R, Wang L, Lei Z-K et al (2018) Study on bending damage and failure of basalt fiber reinforced concrete under freeze-thaw cycles. Constr Build Mater 163:460–470. https://doi.org/10.1016/j.conbuildmat.2017.12.096
141. Zhong H, Zhang M (2020) Experimental study on engineering properties of concrete reinforced with hybrid recycled tyre steel and polypropylene fibres. J Clean Prod 259:120914. https://doi.org/10.1016/j.jclepro.2020.120914
142. Zhong R, Wille K (2015) Material design and characterization of high performance pervious concrete. Constr Build Mater 98:51–60. https://doi.org/10.1016/j.conbuildmat.2015.08.027
143. Zieliński K, Olszewski P (2005) Der Einfluss von Basaltfasern auf ausgewählte physische und mechanische Eigenschaften von Zementmörtel. Betonwerk und Fertigteil-Technik/Concrete Precasting Plant and Technology

Figures

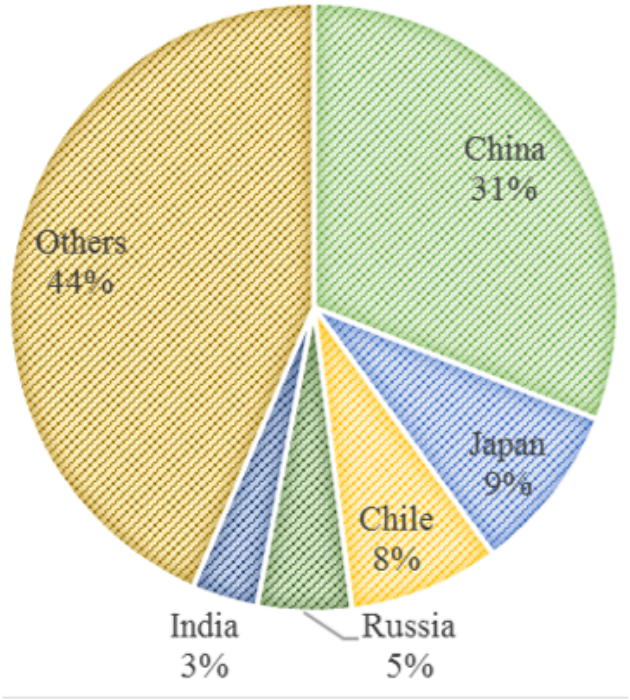

Figure 1

Copper slag rates released around the world in 2015 (International Copper Study Group 2016)

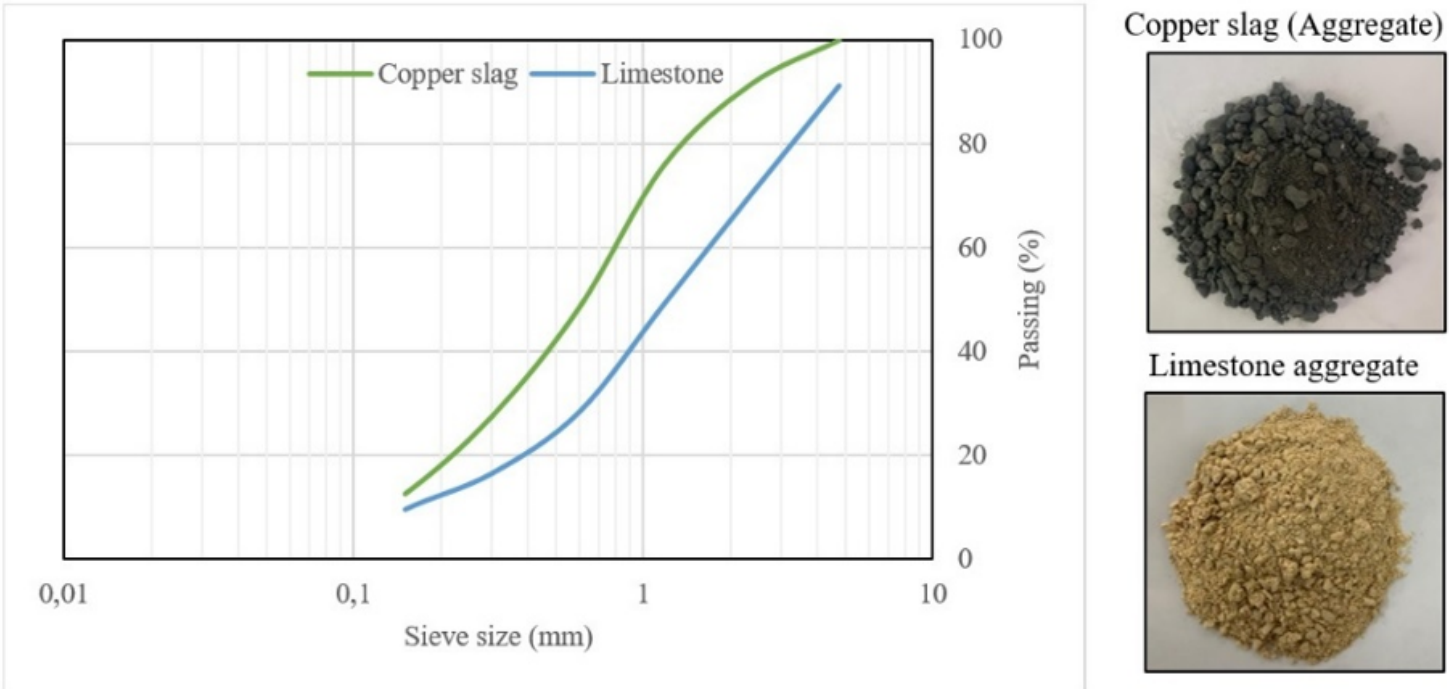

Figure 2

Particle distribution and appearances of the aggregates

(a) Ball mill (for cement)

(b) Stone Crusher (for aggregate)

Figure 3

Equipment used in copper slag processing

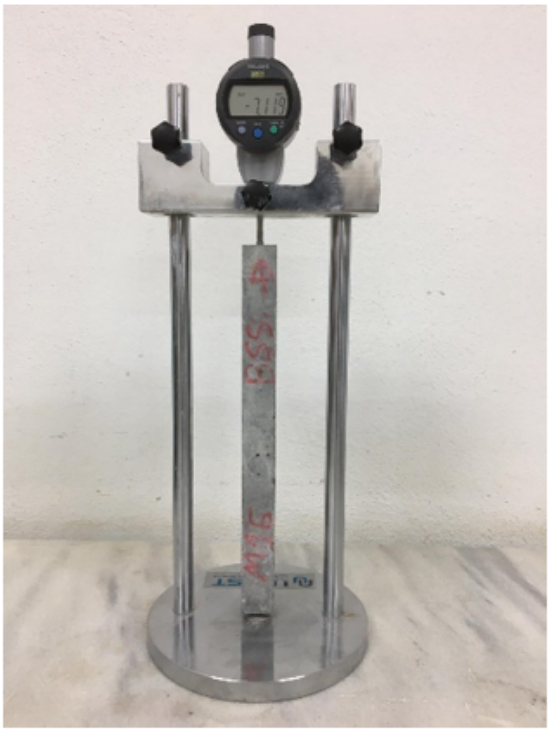

Figure 4

Digital comparator used to determine length changes

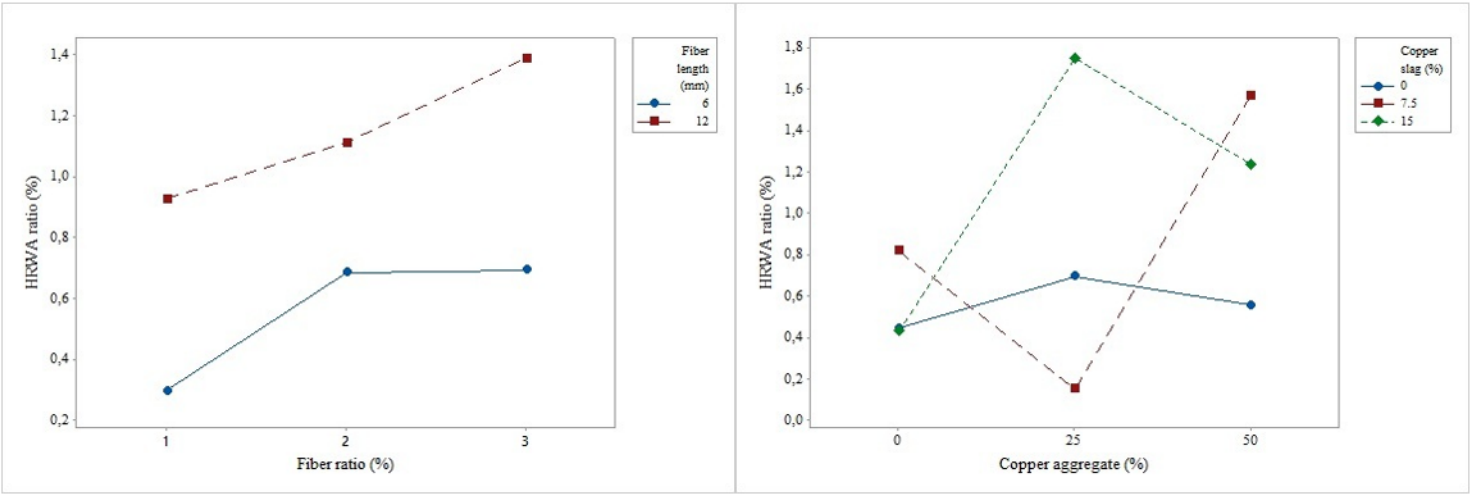

(a) Effect of basalt fiber (b) Effect of copper waste

Figure 5

Plasticizer ratios used in cement based composites

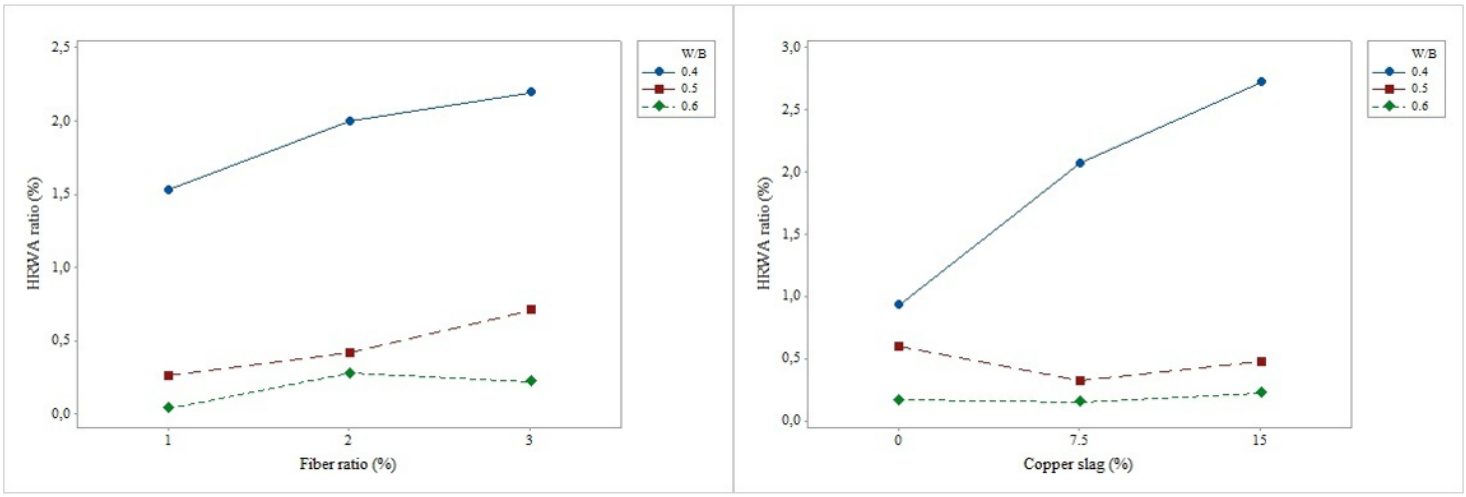

(a) Effect of fiber ratio (b) Effect of copper slag ratio

Figure 6

The effect of different w/b ratios on the plasticizer ratio in cement based composites.

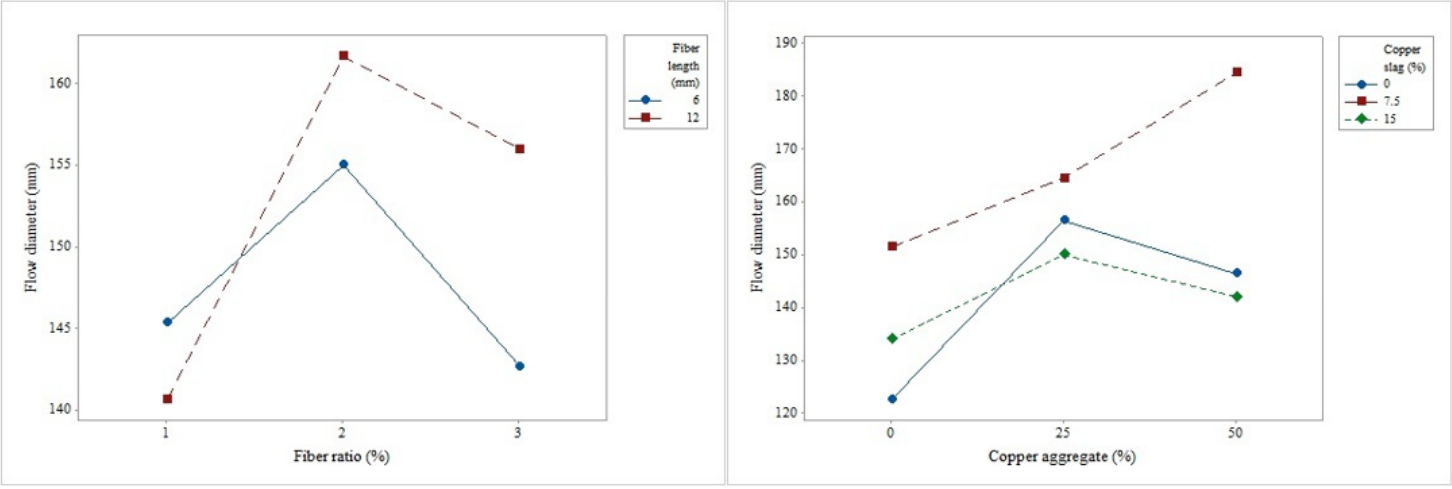

(a) Effect of basalt fiber (b) Effect of copper waste

Figure 7

Flow diameter of cement based composites

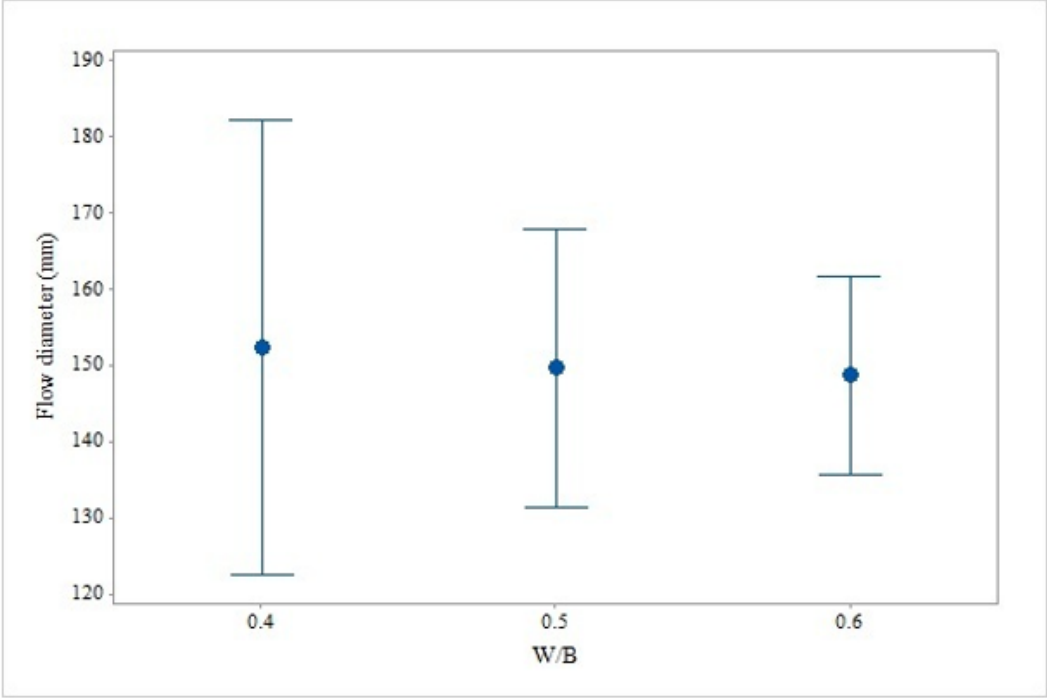

Figure 8

Effect of W/B ratio on flow diameter

Figure 9

Fresh state properties of cement based composites

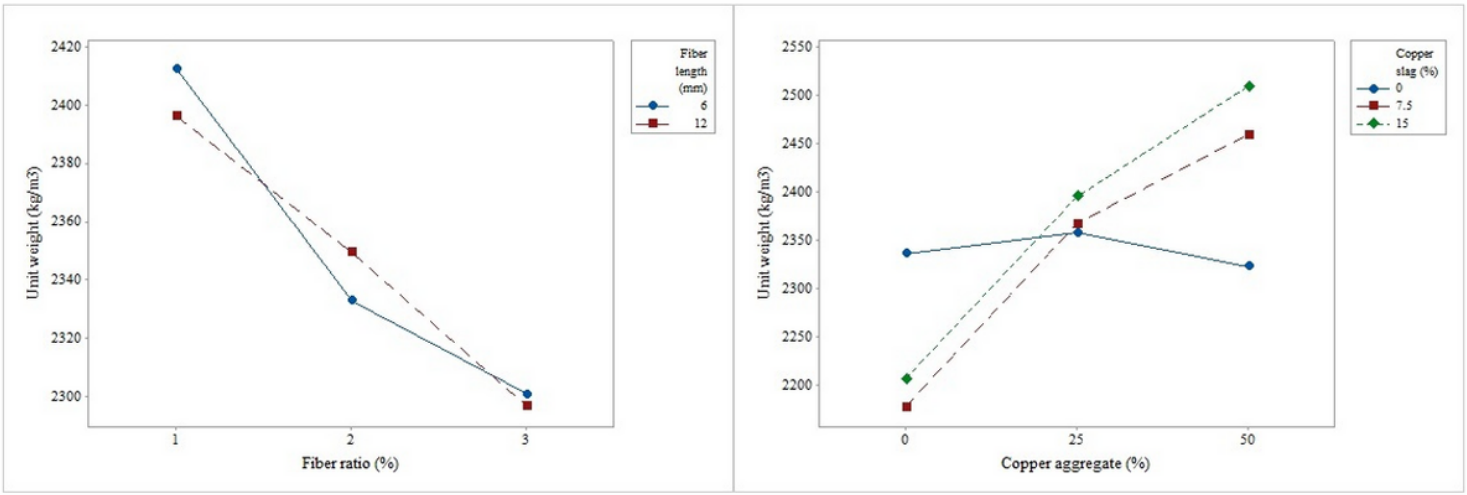

(a) Effect of basalt fiber (b) Effect of copper waste

Figure 10

Unit weight values of cement based composites

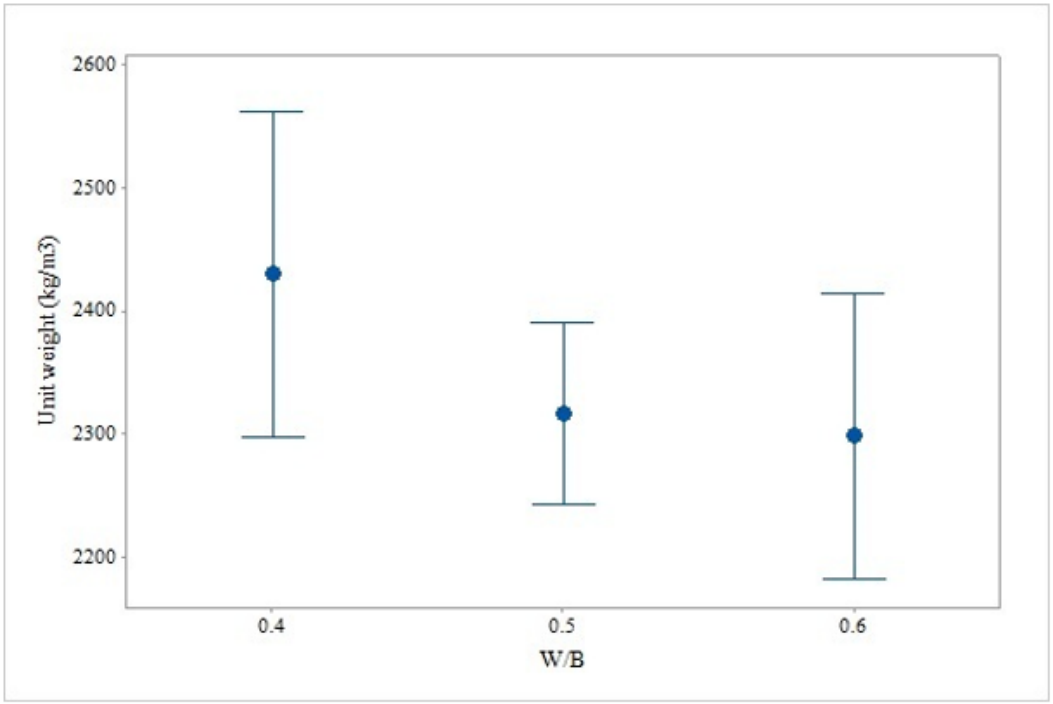

Figure 11

Effect of W/B ratio on unit weight

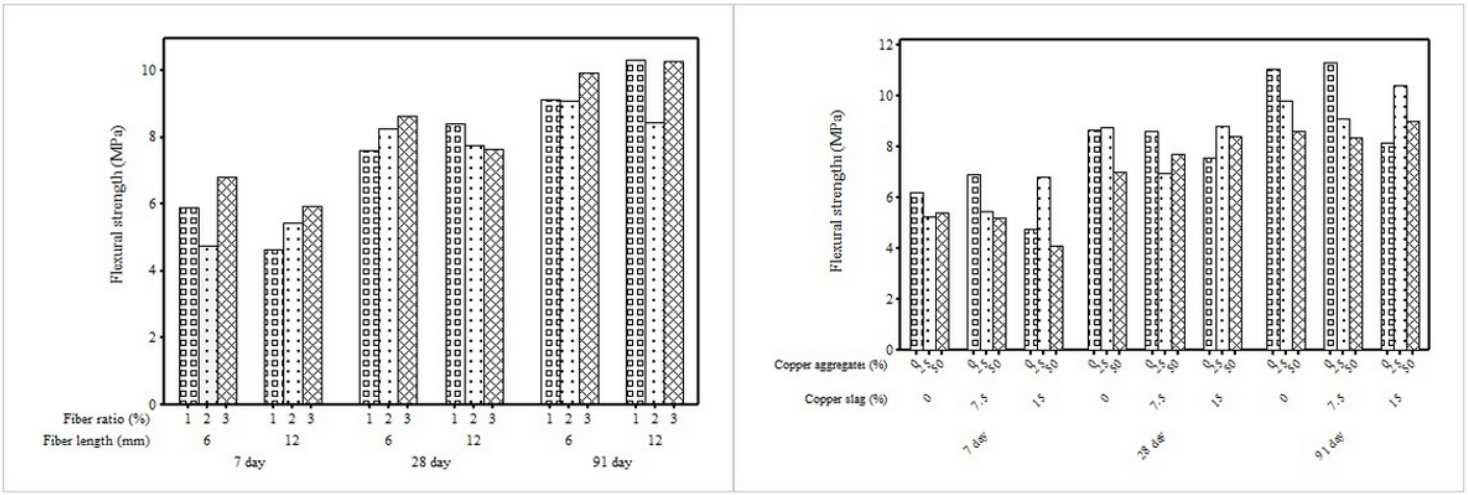

(a) Effect of Basalt fiber (b) Effect of Copper waste

Figure 12

Flexural strength of cement-based composites

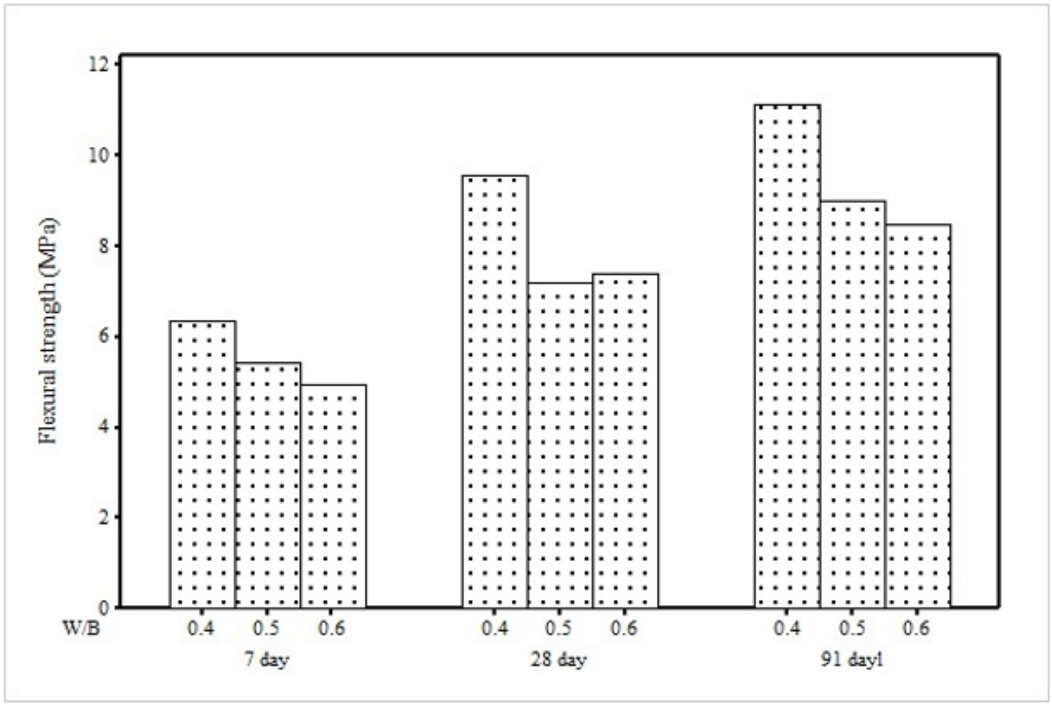

Figure 13

The effect of W/B ratio on flexural strength

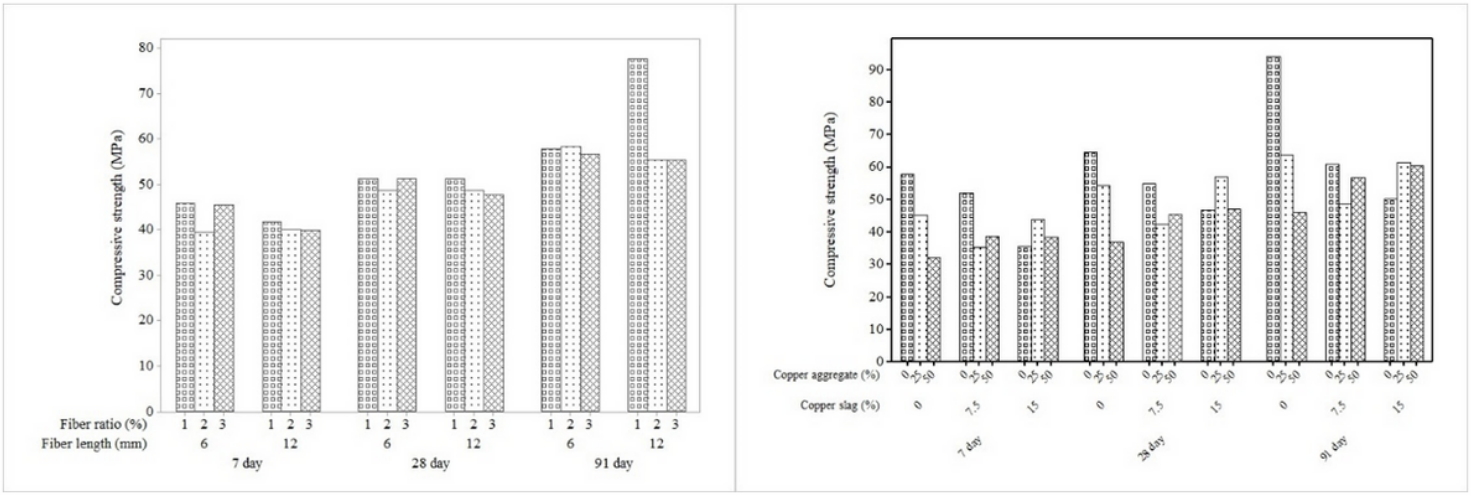

Figure 14

Compressive strength of cement based composites

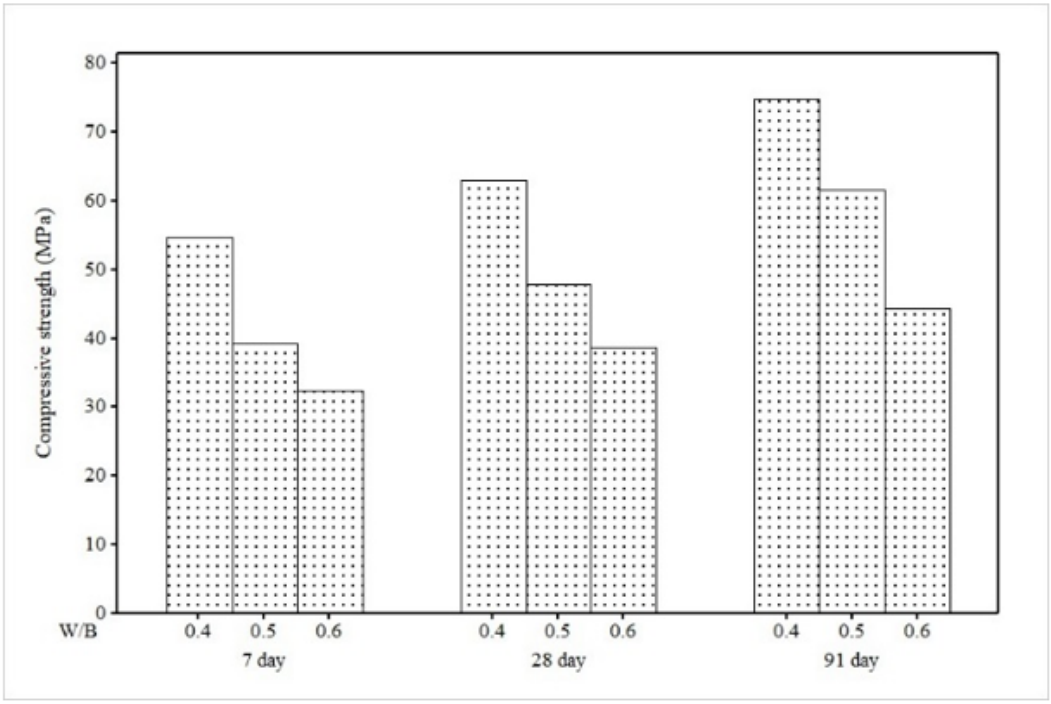

Figure 15

The effect of W/B ratio on compressive strength

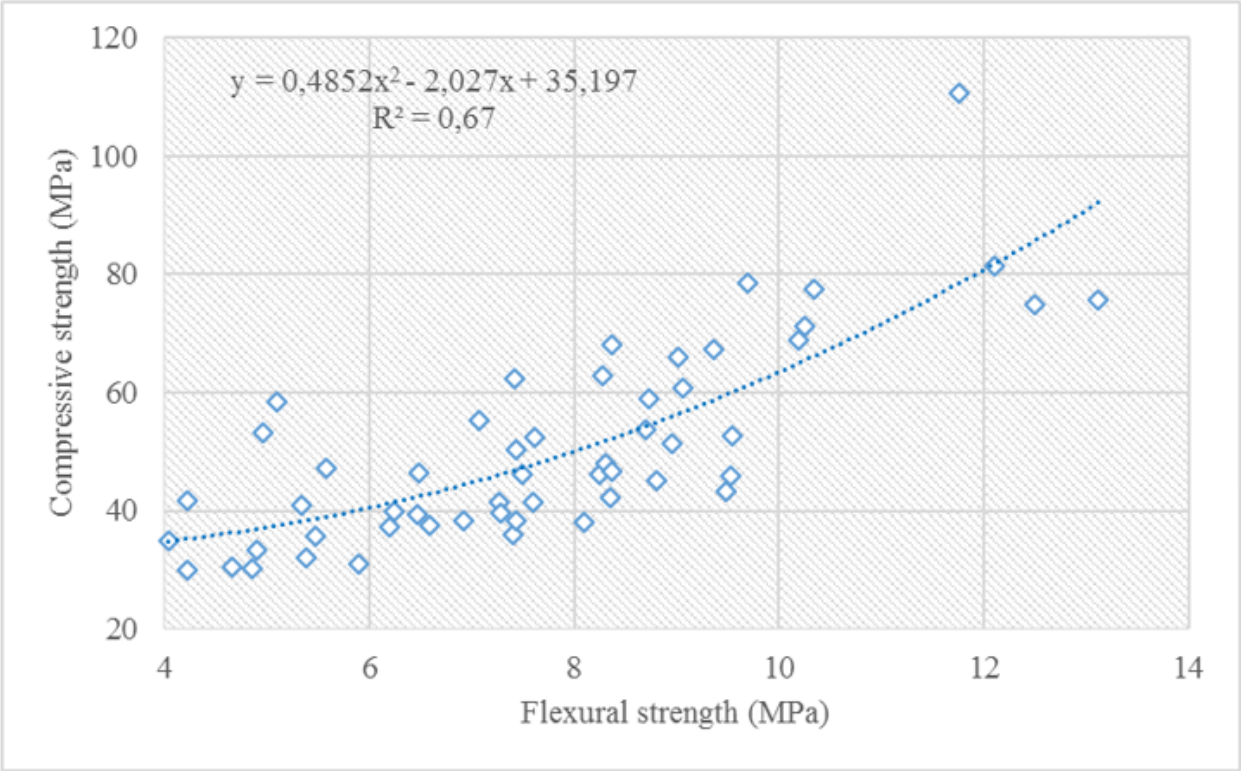

Figure 16

Relationship between compressive and flexural strength

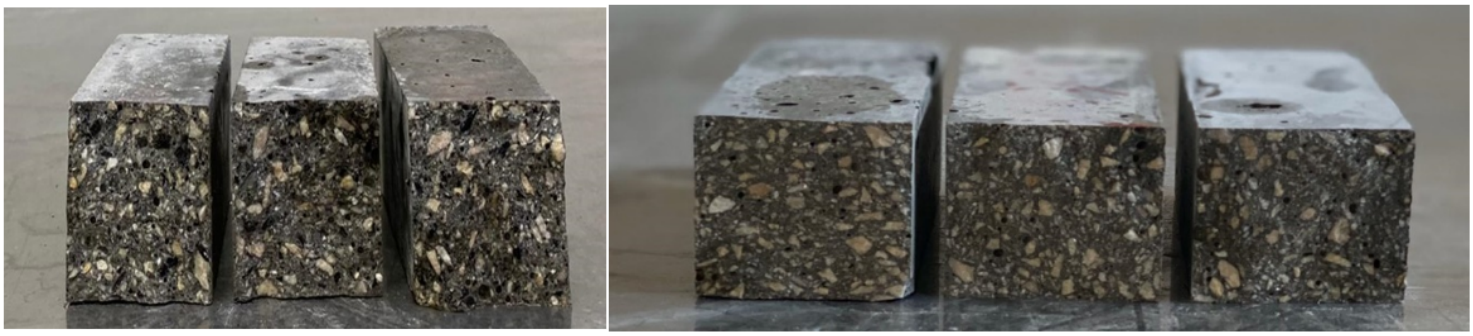

(a) Samples with copper aggregate (b) Samples without copper aggregate

Figure 17

Aggregate distribution in cement based composites

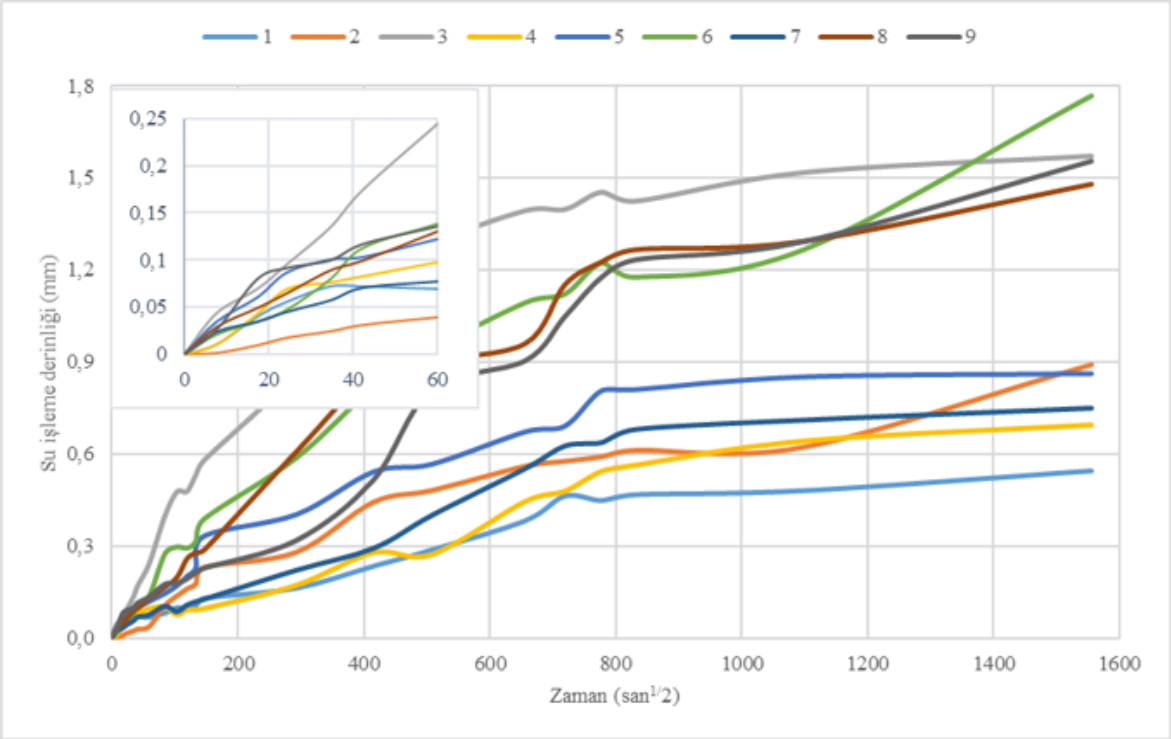

Figure 18

Sorptivity properties of mixtures produced from 6 mm long fibers

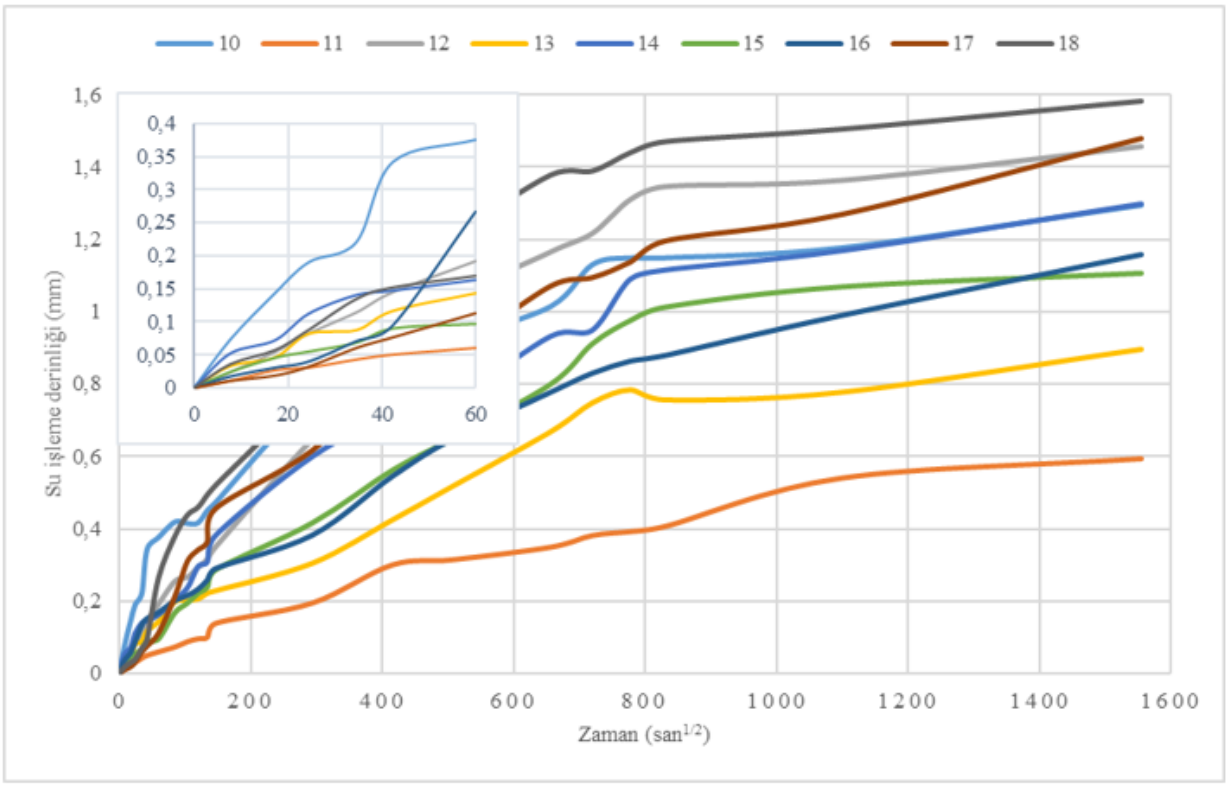

Figure 19

Sorptivity properties of mixtures produced from 12 mm long fibers

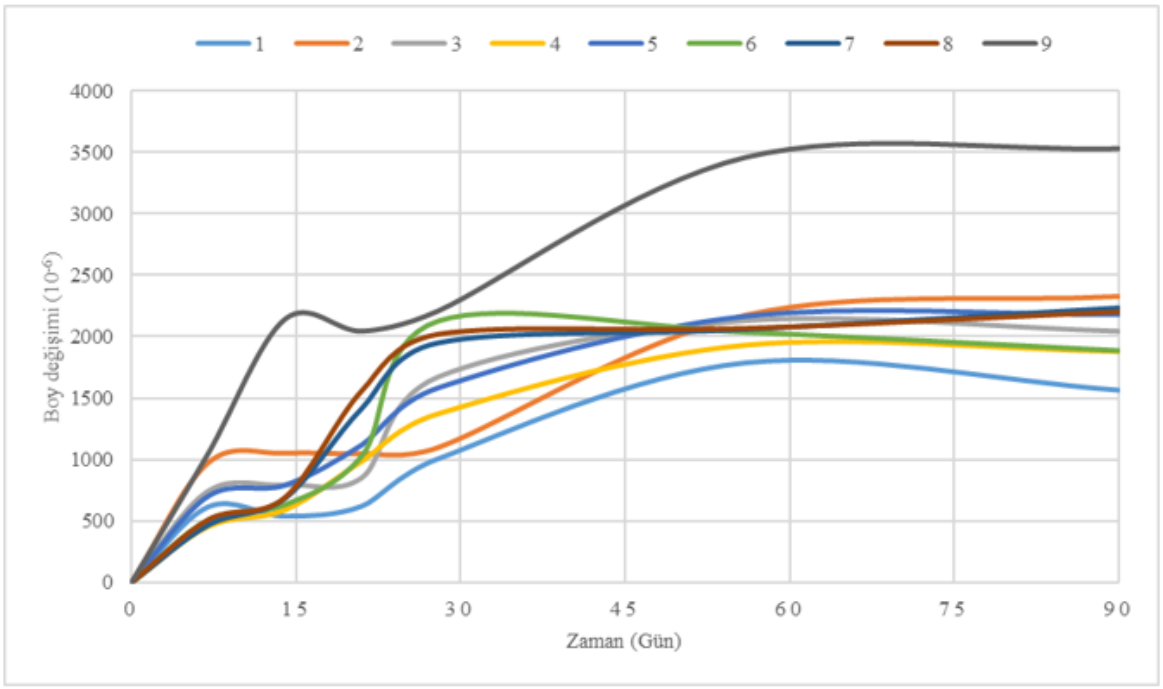

Figure 20

Drying shrinkage properties of mixtures produced from 6 mm long fibers

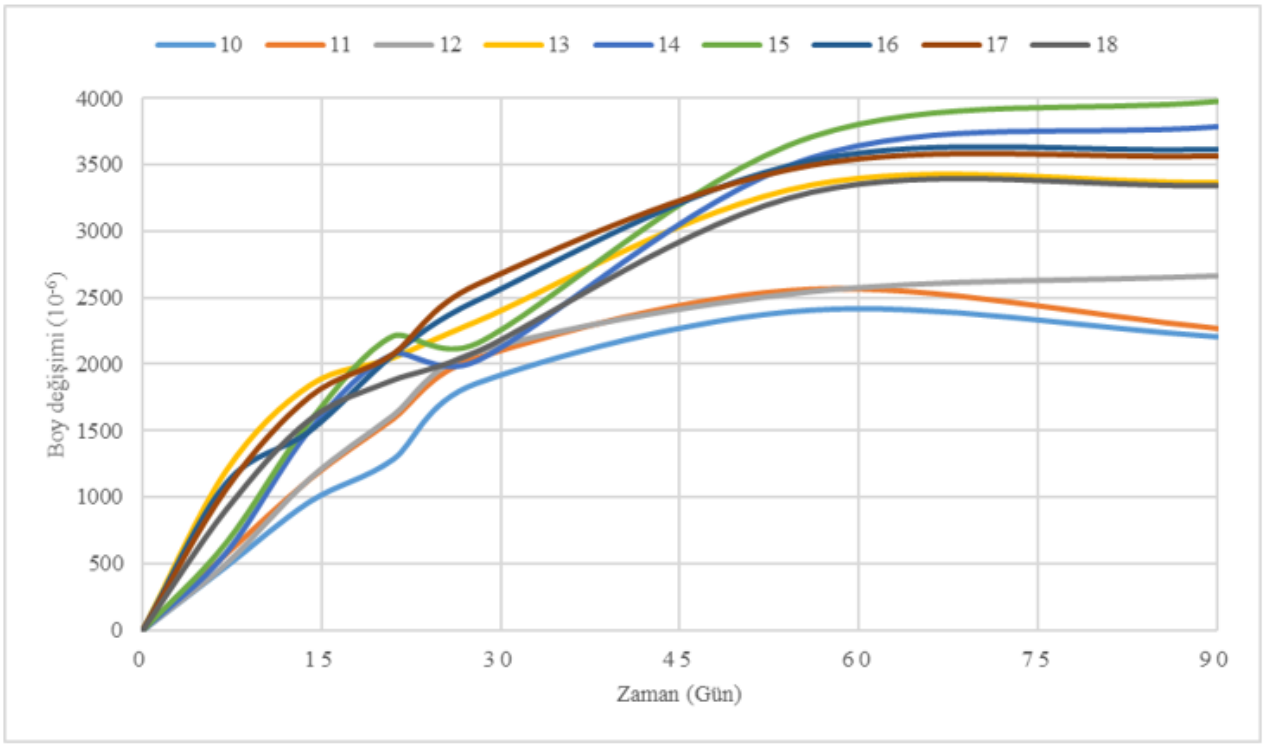

Figure 21

Drying shrinkage properties of mixtures produced from 12 mm long fibers.

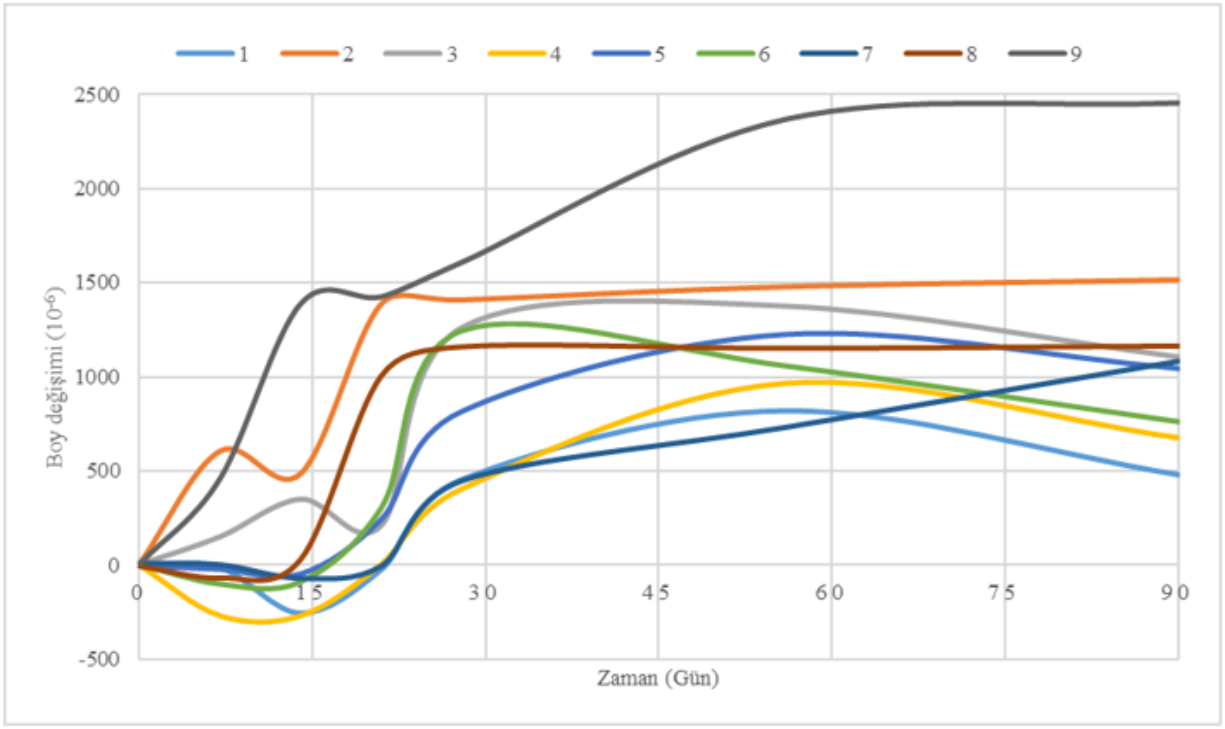

Figure 22

Sulphate expansion of mixtures produced from 6 mm long fibers.

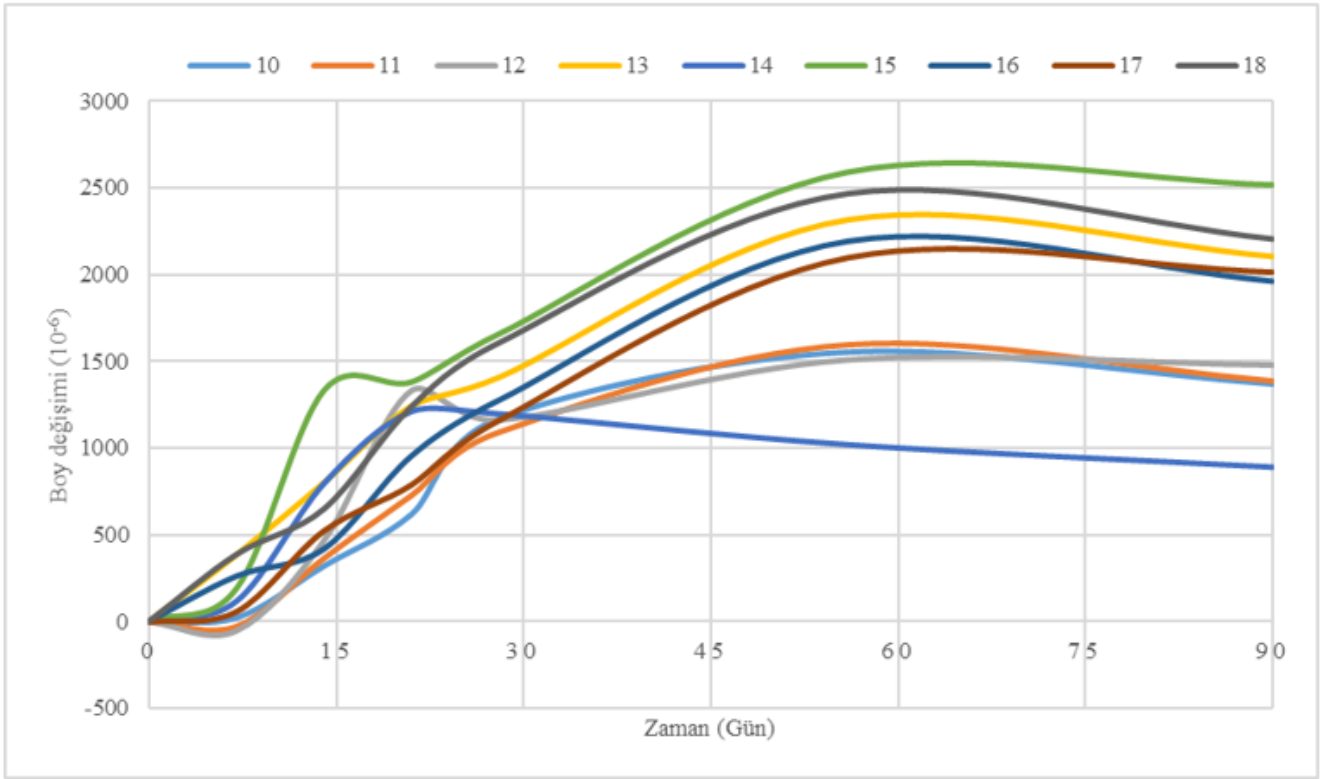

Figure 23

Sulphate expansion of mixtures produced from 12 mm long fibers.

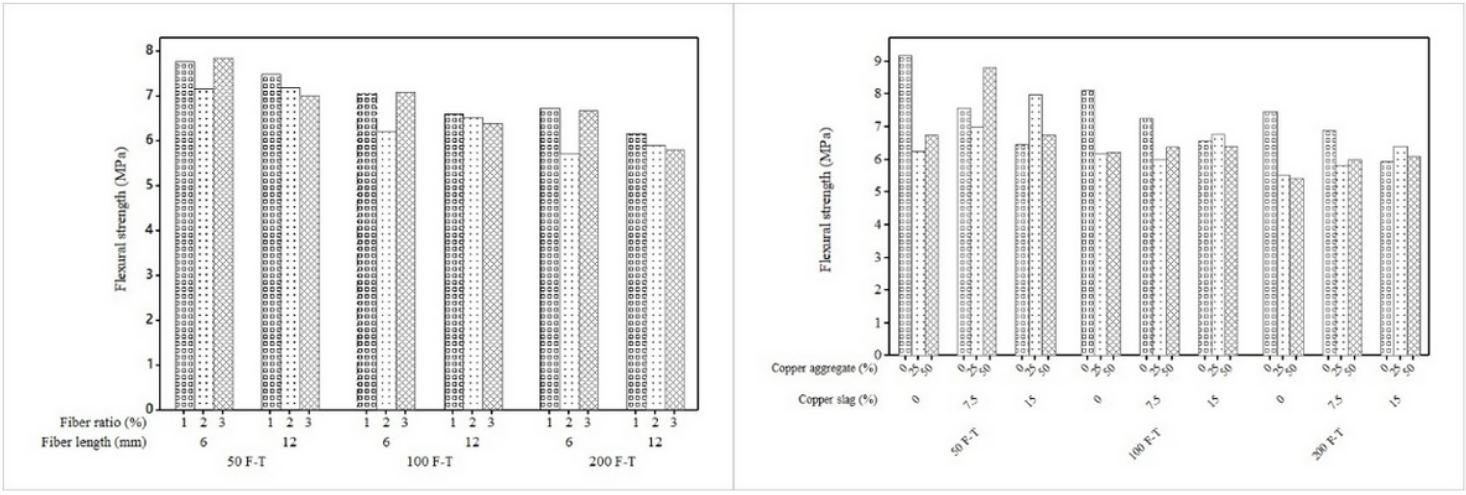

(a) Effect of basalt fiber (b) Effect of copper waste

Figure 24

Flexural strength of cement based composites after freeze-thaw

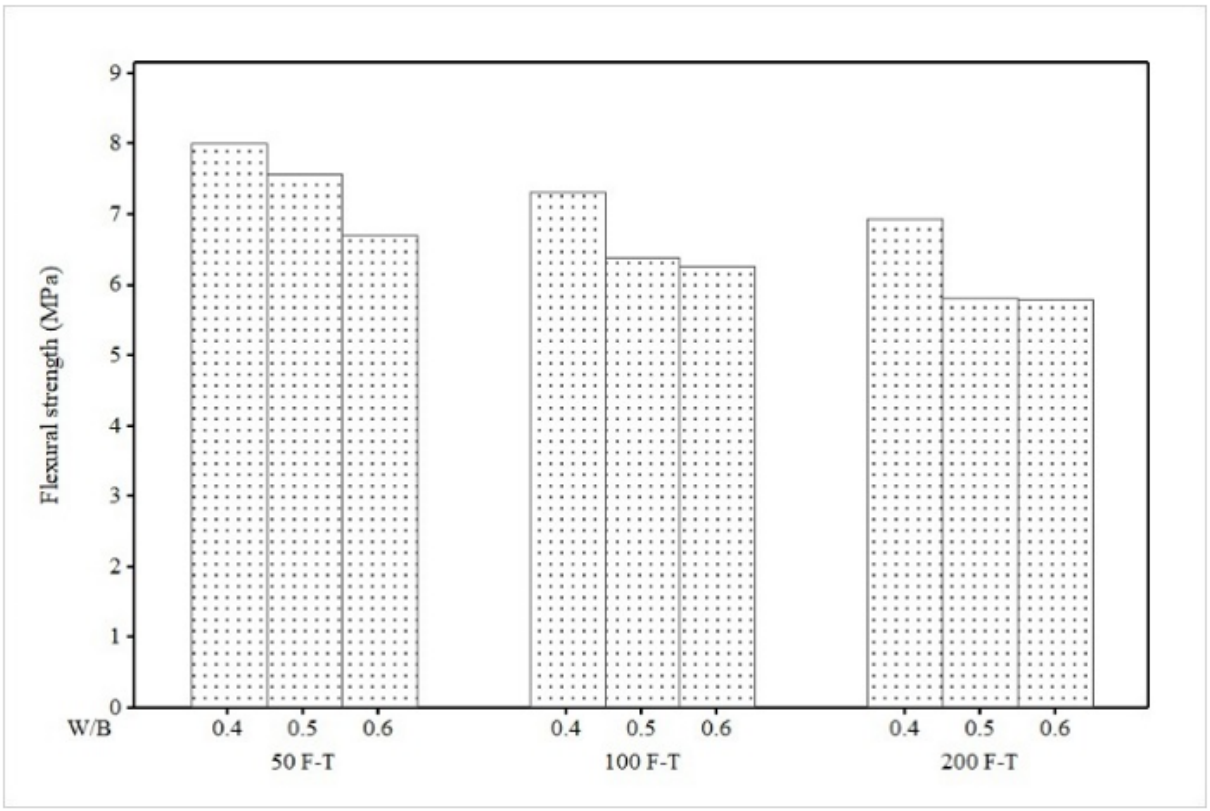

Figure 25

The effect of W/B effect on flexural strength after freeze-thaw

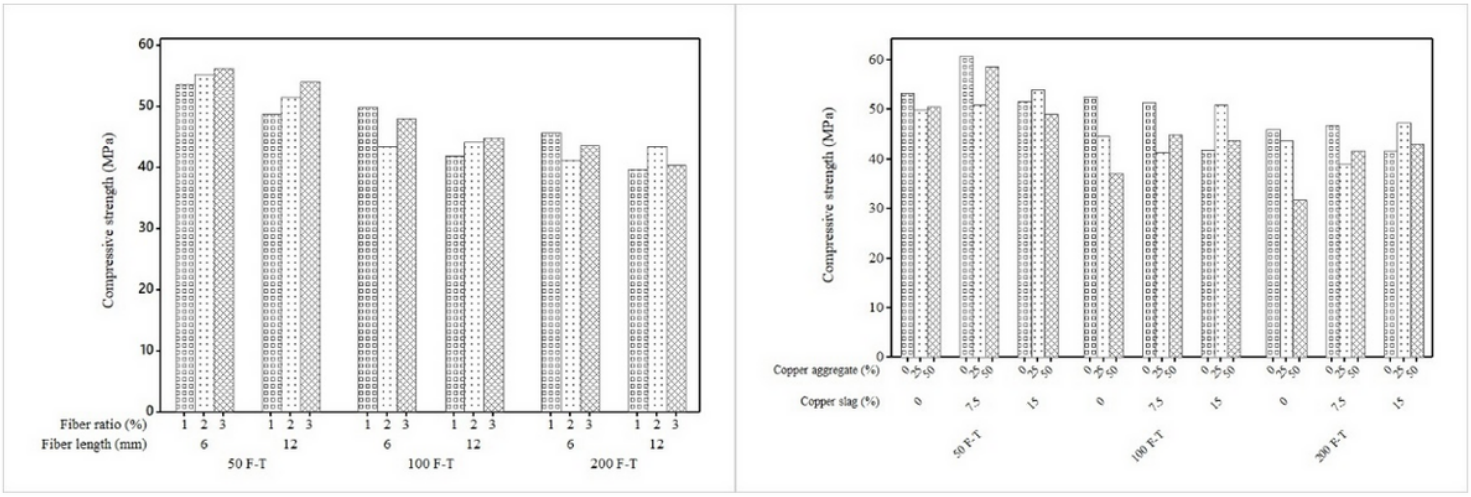

(a) Effect of Basalt fiber (b) Effect of Copper waste

Figure 26

Compressive strength of cement based composites after freeze-thaw

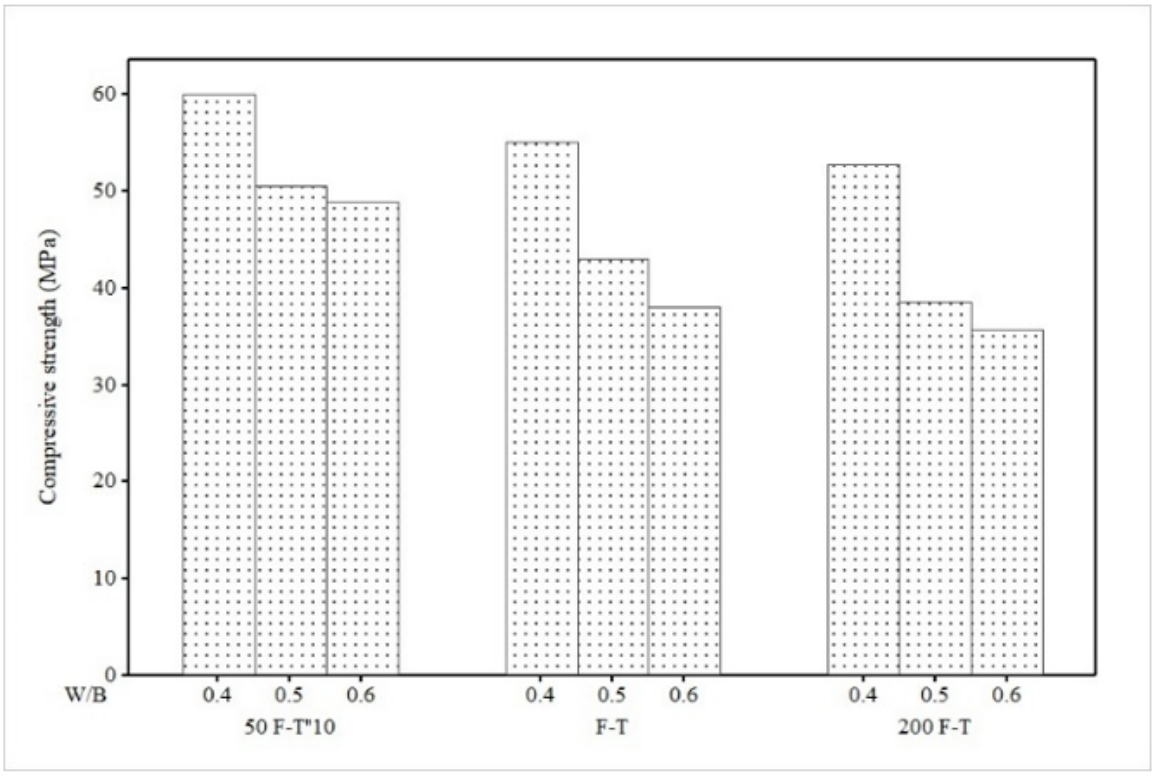

Figure 27

The effect of W/B effect on compressive strength after freeze-thaw

Figure 28

Damages that can be observed in some samples after 200 F-T cycles